RIZA
Documentatie
Postbus 600
8200 AP LELYSTAD
Nederland

A083914838 ISN: 744939 PERIODIEK **OPGEHAALD** 2007-01-31

Verzoeke te behandelen voor: 14-02-2007 **Ingediend door:** 0510 **Datum en tijd van indienen:** 31-01-2007 13:23 **Datum plaatsen:** 31-01-2007 13:23
Type aanvrager: overige (non-profit) **t.a.v.:** Bibliotheek **I.D.:** BIBLIOTHEEK

PPN: 861186605

Water resources research American Geophysical Union 200X Washington, D.C. American Geophysical Union

Gewenst: 1993-00-00 **Deel:** 29 **Nummer:** 3 **Electronisch leveren ()**

Auteur:	**Titel van artikel:**	**Pagina's:**
Jensen, K.Hgh (ed.)	Large-Scale Dispersion Experiments in a Sandy Aquifer in Denmark: Obser	673-696

Opmerking:
aanvr. 24

METEO	Hdb 4	muurkast	Vol. 17(1981)-18(1982)
HAAFF	MAG	NN44568	Vol. 1(1965)-40(2004)
HAAFF		KELDER	Vol. 8(1972)-40(2004)
WWW			Vol. 41(2005)-

1. ○ origineel gestuurd
2. ○ fotokopie gestuurd
3. ○ overige
4. ○ nog niet aanwezig
5. ○ niet aanwezig
6. ○ niet beschikbaar
7. ○ uitgeleend
8. ○ wordt niet uitgeleend
9. ○ bibliografisch onjuist
10. ○ bij de binder

Fakturen zenden aan: OCLC PICA B.V.
T.a.v. Depositobeheer
Postbus 876
2300 AW Leiden

WATER RESOURCES RESEARCH, VOL. 29, NO. 3, PAGES 673–696, MARCH 1993

Large-Scale Dispersion Experiments in a Sandy Aquifer in Denmark: Observed Tracer Movements and Numerical Analyses

K. HØGH JENSEN AND K. BITSCH

Institute of Hydrodynamics and Hydraulic Engineering, Groundwater Research Centre Technical University of Denmark, Lyngby

P. L. BJERG

Department of Environmental Engineering, Groundwater Research Centre, Technical University of Denmark, Lyngby

A large-scale natural gradient dispersion experiment was carried out in a sandy aquifer in the western part of Denmark using tritium and chloride as tracers. For both plumes a marked spreading was observed in the longitudinal direction while the spreading in the transverse horizontal and transverse vertical directions was very small. The horizontal transport parameters of the advection-dispersion equation were investigated by applying an optimization model to observed breakthrough curves of tritium representing depth averaged concentrations. No clear trend in dispersion parameters with travel distance for distances between 50 and 200 m could be found, suggesting that the asymptotic stage was reached within a short distance from the point of injection. A three-dimensional numerical model for flow and transport was applied to the aquifer in order to quantify the dispersivity parameters more closely. The following "best fit" dispersivity parameters were identified: longitudinal horizontal, 0.45 m; transverse horizontal, 0.001 m; and transverse vertical, 0.0005 m.

1. INTRODUCTION

Transport behavior of nonreactive solutes in groundwater is generally considered to be governed by the two principal processes: advection and dispersion, which describe the role of hydrodynamics in transport and dilution of soluble substances. Advection refers to the mean movement of the solute in the flowing groundwater, while dispersion describes the solute spreading about the mean motion caused by local fluctuations in velocity [*Freeze and Cherry*, 1979].

The classical model of transport in groundwater is the advection-dispersion equation, in which dispersion is considered to be analogous to a Fickian diffusion process [*Bear*, 1972]. This model was originally developed at the scale of a representative elementary volume, where the dispersion parameter, the dispersivity, is regarded as a unique and measurable property of the medium at the pore-scale continuum. However, the model has been widely applied to large-scale regional transport problems simply by amplifying the dispersivity parameter in order to account for the enhanced mixing caused by the heterogeneity of the hydraulic properties in aquifer systems. In this way the dispersivity has essentially been used as a lumped parameter which accounts for all the unknown fluid velocity variations related to the aquifer heterogeneity.

The dispersivity is usually determined by calibration of the advection-dispersion model to observed concentrations. In practical contamination situations, sufficient concentration data will generally not be available for a reliable determination of the dispersivity, and furthermore, the history of the contamination source is often unknown, which implies that the value obtained by calibration becomes very uncertain.

Analyses of solute behavior in natural field environments have indicated that the dispersive spreading and dilution behave in a non-Fickian manner over the initial travel distances from the source, and that the dispersivity increases with the scale of the transport distance (see, for example, discussions by *Anderson* [1979] and *Gilham and Cherry* [1982]). Various reviews and compilations of field-scale observations of longitudinal dispersivities [*Lallemand-Barres and Peaudecerf*, 1978; *Gelhar et al.*, 1985; *Kinzelbach*, 1986] have shown the scale effect, and furthermore, it has been shown that the dispersivity exhibits a wide range of variation for the same type of aquifer and transport distance. The physical explanation of these phenomena is that with increasing travel distance the contaminant plume is exposed to more and more aquifer heterogeneity, and consequently, larger dispersive mixing takes place.

Theoretical studies of contaminant transport have emphasized the significance of spatial variability of hydraulic conductivity and the uncertainty always encountered when a mapping of aquifer properties is attempted. By treating the natural heterogeneity in a stochastic sense, stochastic forms of the groundwater flow and transport equations have been developed in which the hydraulic parameters appear as random variables. These studies including those by *Gelhar et al.* [1979], *Matheron and de Marsily* [1980], *Smith and Schwartz* [1980], *Dagan* [1982, 1984], and *Gelhar and Axness* [1983] have demonstrated the influence of hydraulic conductivity variations on dispersive mixing.

As mentioned above, field observations on dispersion behavior have been reported in the literature, but as pointed out by *Gelhar et al.* [1985], the reliability of many of the reported dispersivities can be questioned. Four comprehensive and rather unique large-scale tracer tests can be mentioned: Borden Air Force Base [*Mackay et al.*, 1986; *Freyberg*, 1986; *Sudicky*, 1986], Cape Cod [*Garabedian et al.*, 1988; *LeBlanc et al.*, 1991; *Garabedian et al.*, 1991], Twin Lake [*Killey and Moltyaner*, 1988; *Moltyaner and Killey*,

Paper number 92WR02468.
0043-1397/93/92WR-02468$05.00

1988*a*, *b*], and Columbus Air Force Base [*Boggs et al.*, 1992]. By establishing very detailed information on the hydrogeological conditions and the spreading patterns of solutes, these field tests have provided new insight into the dispersion process, and they have also served the purpose of providing validation data for the stochastic theories. However, in none of these studies to date was a three-dimensional deterministic model analysis of the plume movements attempted.

The purposes of the study reported here were to carry out a tracer experiment at a site extensively equipped with observation piezometers in order to (1) examine the dispersion processes in a sandy aquifer typical of the geological conditions in the western part of Denmark; (2) determine the dispersivity parameters of the aquifer; (3) compare with the dispersivity parameters determined from the statistical properties of the hydraulic conductivity variation; and (4) produce a detailed and accurate data base for validation of three-dimensional numerical models of groundwater flow and tracer transport.

Two natural gradient tests were performed using tritium and chloride as tracers applied in two different injection modes. The present tracer tests involve other combinations of geological and experimental conditions than reported previously and will as such complement the other tests mentioned above.

In this paper we describe the experimental site and conditions under which the tracers were applied, sampled, and analyzed. The geological and hydrogeological conditions are discussed, and investigations of the hydraulic conductivity distribution are summarized. The results of the tracer experiments are illustrated as horizontal and vertical distributions at different times during the development of the plumes. The transport parameters are evaluated from the data. Finally, we introduce a three-dimensional numerical finite difference model for nonsteady flow and transport. Simulation results are illustrated and compared to measurements of water table fluctuations and tracer concentrations.

2. AQUIFER CHARACTERISTICS

2.1. *Geological Conditions*

The experimental site (200 m × 40 m) is located in the western part of Denmark on the Jutland peninsula (Figure 1). The area was formed during the latest glacial period by a river system carrying meltwater and sediments from a glacial front located in the middle of the peninsula in a north-south direction. A huge outwash plain was created to the west composed of layers of fine-grained, medium-grained, and coarse-grained sand depending on the settling conditions which prevailed at the individual locations. Although the aquifer is generally considered to be fairly homogeneous, discontinuous lenses of coarser grained sand as well as silty formations have been observed which may be of importance for the transport behavior of the tracers.

The local geology at the experimental site has been described by *Bjerg et al.* [1992] on the basis of 31 sediment cores. A low-permeable clay layer at approximately 10 m depth defines the lower boundary of the aquifer. The surface of this layer undulates between elevations 30 and 31 m except at the distance of 135–155 m downgradient from the injection wells (see Figure 1) where the clay surface dips. In general, a shallow 5-m-thick aquifer horizon is available for the tracer experiment.

2.2. *Hydraulic Parameters*

The spatial distribution of the hydraulic conductivity was determined by performing slug tests in the three-dimensional network of separate sampling wells (2.5 cm diameter and 0.25-m screen) shown in Figure 1. A single-well response test was carried out in the individual wells (110 locations at 1–10 depths for a total of 334 tests) by raising the water level in the well 1–2 m above the initial groundwater level using a vacuum pump. After equilibrium was achieved the vacuum was released and the rate of decline of the water level monitored. The falling-head data were analyzed, and the hydraulic conductivity was derived using the method developed by *Dax* [1987]. The experimental procedure has been reported by *Hinsby et al.* [1992].

Basic statistical and geostatistical analyses were carried out and reported by *Bjerg et al.* [1992]. In Table 1 some of these results are summarized both on a global basis and for three structural layers. These layers were identified on the basis of a geological analysis of sediment cores and by analyzing the vertical variation of the hydraulic conductivity (data available at 0.5 m intervals) [*Bjerg et al.*, 1992]. Slight but noticeable differences are present in the statistical parameters between the three layers.

The hydraulic conductivity K has a global geometric mean of 5.1×10^{-4} m/s and a ln K variance of 0.37 assuming a lognormal distribution. Note that the mean value falls between the Borden Site value of 9.75×10^{-5} m/s [*Sudicky*, 1986] and the Twin Lake value of about 2.0×10^{-4} m/s [*Killey and Moltyaner*, 1988] on one side and the Cape Cod Site value of 1.4×10^{-3} m/s [*Garabedian et al.*, 1988] on the other, while the ln K variance of 0.37 corresponds closely to the Borden Site. All of these test field sites have a ln K variance much less than the site at Columbus Air Force Base [*Boggs et al.*, 1992].

The horizontal correlation length of ln K is estimated to be in the range of 1.0 to 2.5 m assuming horizontal isotropy. This value corresponds to the correlation length of 2.8 m found at the Borden Site [*Sudicky*, 1986] which has a comparable geological history.

The total porosity was obtained from measurements on sediment samples and by cone penetration tests, while the effective or dynamic porosity was estimated from the observed travel velocity of the tracer clouds.

2.3. *Groundwater Flow System*

The groundwater flow in the study area occurs under unconfined conditions and the average water table depth is approximately 5.0 m below the land surface.

The groundwater is recharged by precipitation in excess of evapotranspiration from the grass-covered area. During the period of investigation (March 1989 to March 1990) the recharge was estimated to be about 350 mm/yr based on simulations using a one-dimensional unsaturated flow model developed by *Jensen* [1983]. The recharge varied over the seasons, which imposed fluctuations in the water table.

The water table configuration was measured regularly during the investigation period using the network of piezometers shown in Figure 1. Seasonal fluctuations of about 1.0 m

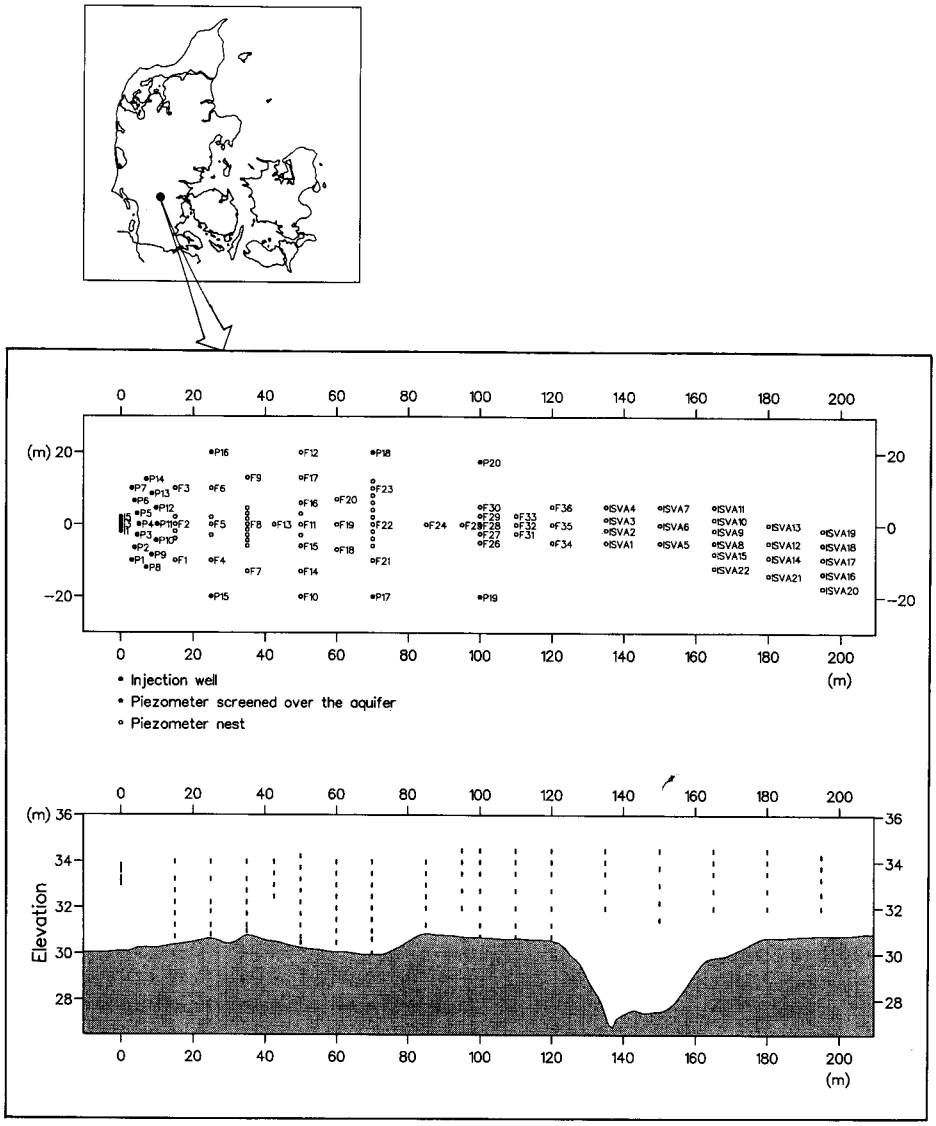

Fig. 1. Plan diagram of sampling locations and cross-sectional diagram of screens along plume trajectory.

were observed with highest levels in early spring and lowest levels in late fall. The fluctuations over a 1-year period for selected wells are shown in Figure 2. All piezometers shown responded similarly to the seasonal changes in recharge, and no significant phase differences were observed. Hence the flow directions are supposed to remain fairly stationary, and transients in flow behavior are expected to have only a minor influence on the dispersion process.

Vertical head gradients were very small. The differences in piezometric levels observed were within the range of measurement and leveling errors. In Figure 2 a water table configuration map established on the basis of measurements from February 14, 1990, is shown, and this configuration therefore essentially represents the flow conditions prevailing over the test period as well as over the aquifer depth. The dominant flow direction conformed rather closely to the orientation of the field site. Furthermore, the diagram seems to indicate that the hydraulic gradient was fairly uniform

TABLE 1. Hydraulic Parameters for Three Structural Layers of the Aquifer

Level, m	K_g, m/s	Range of Variation of K, m/s	$\sigma^2_{\ln K}$	$\lambda_{\ln K}$, m	n	n_e
33.0–34.5	5.6×10^{-4}	$1.3–15.7 \times 10^{-4}$	0.20	2.5	0.38	0.30
32.0–33.0	4.4×10^{-4}	$0.8–12.3 \times 10^{-4}$	0.41	1.0	0.38	0.30
31.0–32.0	6.1×10^{-4}	$1.6–22.5 \times 10^{-4}$	0.29	1.0	0.38	0.30
global	5.1×10^{-4}		0.37			

K_g is geometric mean of hydraulic conductivity, $\sigma^2_{\ln K}$ is variance of ln K, λ is horizontal correlation length of ln K, n is full porosity, and n_e is estimated effective porosity.

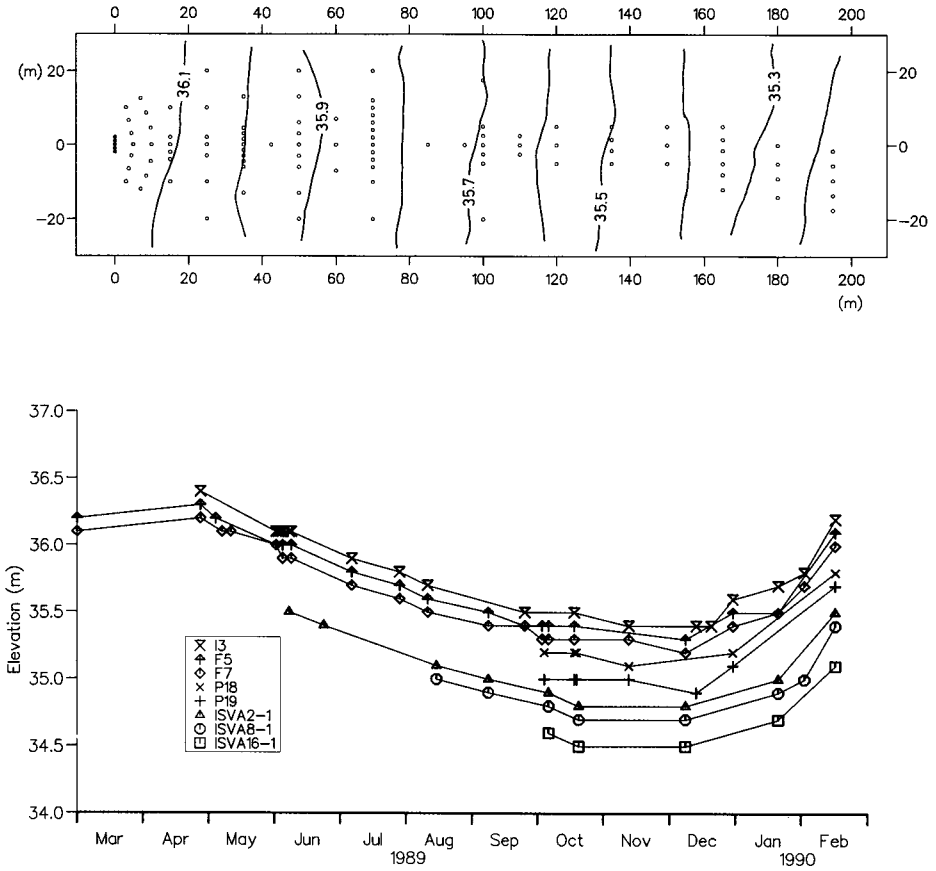

Fig. 2. Water table configuration (February 14, 1990) and seasonal fluctuations of the water table in observation wells along the longitudinal direction.

over the area (4.5‰ on the average) thus suggesting that the hydraulic properties are rather uniform.

3. Experimental Procedure

3.1. *Site Layout and Sampling Structure*

A 200-m-long and 40-m-wide area was allocated for the experiment oriented with the longest side parallel to the prevailing groundwater flow direction. The monitoring system consisted of a dense network of piezometers with screens at various levels installed concurrently with the development of the plumes. Figure 1 shows a plan diagram of the sampling network involving a total of approximately 100 sampling locations, and a diagram of the screens in a cross section placed along the trajectory of the plumes. As is shown in Figure 1, up to nine screens could be present in a given vertical. At the edges of the plumes the number of screens was less than shown in Figure 1. The horizontal spacing of the multilevel sampling locations varied from 5 to 15 m in the longitudinal direction and most typically from 1 to 5 m in the transverse direction. The vertical spacing of the sampling ports was typically 0.5 m along the trajectory of the plumes.

All sampling piezometers were established in separate wells to avoid cross-contamination during sampling. The installation was accomplished by driving the piezometer tube to the desired level. Some piezometers were established by driving a casing into the soil and subsequently installing a 1.6-cm polyvinyl chloride (PVC) tube with a slot screen at the bottom followed by withdrawal of the casing. Other sampling tubes were made of 2.5-cm-diameter iron metal with a screen of rigid metal net at the bottom which enabled them to be driven directly to the desired depth. All piezometers were equipped with 25-cm screens. The injection wells were of a larger diameter (5 cm) with 50-cm screens. The piezometers installed in a semicircle arrangement near the injection wells (see Figure 1) were all screened over 1.5 m because they were only used during the very initial phase of the first experiment to make sure that the tracer cloud took the right direction.

3.2. *Tracer Applications*

One objective of the first tracer test was to investigate the physical transport and dispersion behavior over a 200 m range, and hence the tracer should reflect the groundwater flow as accurately as possible. As outlined by, e.g., *Gaspar and Oncescu* [1972], *UNESCO* [1980], and *Davis et al.* [1985], a number of requirements for a field tracer need to be considered. These include high solubility, large contrasts between background and injection concentration, no density effects, no retardation, and measurability at small concentrations. We selected tritium (^3H) as the primary tracer mainly for the contrast and density reasons. Tritium has been viewed as a near-ideal tracer, because it forms part of the water molecule and travels with the groundwater. The major disadvantage is the radiological hazard for which reason careful consideration of the safety aspects is required.

The injection in the first experiment was designed to approximate an instantaneous pulse in a well-defined flow field with minimal disturbance of the natural flow. The tracer was injected in three wells (wells I2, I3, and I4) which were spaced 1 m transverse to the flow direction (Figure 1), each screened over a 0.5-m interval. At the time of injection (March 1, 1989) the screened intervals were located 5.5–6.0 m below ground surface (elevation 33.4–33.9 m) corresponding to 2.4–2.9 m below the water table.

A 50-L solution of 1.55×10^9 Bq ^{3}H was pumped into each of the injection wells over less than 30 min for a total of 4.66×10^9 Bq ^{3}H. The solution volume applied was chosen to ensure that the mass of tritium was distributed properly around the injection wells.

The initial movement of the tritium plume showed very little transverse dispersion and the horizontal transport velocity was very high (~0.8 m/d), which could suggest that the plume was entrapped in a highly permeable layer. In order to investigate whether these observations were representative of the geological conditions at the injection site, it was decided to drive the screens of the injection wells down an additional 0.5 m for the second tracer experiment.

The second experiment was designed to study the ion-exchange processes in the aquifer [*Bjerg and Christensen*, 1993]. Chloride was involved in the experiment and the movement of the chloride plume is analyzed in this paper assuming that this constituent behaves as a nonreactive tracer.

The experiment was carried out by injecting groundwater spiked with sodium chloride (NaCl) and potassium chloride (KCl) continuously over 37 days starting on May 1, 1989. To increase the lateral dimension of the plume five injection wells (wells I1 to I5) with 1 m spacing were used. The average pumping rate was 9.0 L/hour for a total injected volume of 8 m^3 and a total mass of chloride of 48 kg. This corresponded to a chloride concentration of approximately 6000 mg/L. The total mass of the injected compounds was 85 kg for a total concentration of 10,600 mg/L, and the density of the injected fluid was approximately 1.007 g/cm^3 giving a relative density difference of 0.007 at 10°C.

3.3. *Sampling and Analyses*

Water samples were collected up to 4 times a week for tritium analyses and on a daily basis for chloride analysis during the most intensive sampling campaigns of the experiment in order to determine the position of the tracers and to accurately define the breakthrough curves at various locations within the field site.

Sample volumes were extracted by suction using a vacuum pump from the piezometer tubes. The wells were pumped prior to sampling to ensure that the ambient groundwater at the piezometer screen was sampled. Water samples for tritium analysis were pumped directly into 20-mL glass bottles, and the concentrations were measured using direct liquid scintillation on a Packard Pico Flour-water cocktail. Chloride concentrations were determined by a ferricyanide method modified from *American Public Health Association* [1985] using a Technicon Auto Analyzer.

A total of approximately 13,000 water samples were collected of which subsets of 4900 and 4000 were analyzed for tritrium and chloride, respectively.

4. OBSERVED TRACER MOVEMENTS

4.1. *Tritium*

Contour maps of vertically averaged tritium concentrations at 104, 153, 190, and 287 days after injection are presented in Figure 3. The concentrations shown are derived on the basis of the discrete measurements in the screens present at the individual horizontal locations. These measurements are multiplied with the depth intervals they represent and porosity 0.30 to obtain the total mass present over the aquifer depth at a given horizontal location. The total mass is subsequently diluted over a 0.5-m aquifer depth interval which represents the vertical extent of the plume during the initial transport distances to obtain the concentrations shown in Figure 3. Note that the vertical extent of the plume increased later in the experiment, and therefore the concentrations shown are not true representations of the average vertical concentrations within the plume.

The contours shown in Figure 3, which are established by a combination of computer and hand contouring, give a good overview of the overall behavior of the tracer from which it is possible to estimate the mean horizontal velocity and trajectory of the migrating pulse. On the basis of the contour maps the rate of horizontal movement can be estimated to be about 0.75 m/d. The direction of the tracer movement follows the projected path derived from the water table configuration including the slight deflection of the trajectory occurring near the downstream end of the field site (see Figure 2).

A significant spreading in the longitudinal direction is observed, resulting in an ever increasing length of the tracer cloud and decreasing peak concentration. On the other hand, the increase in the lateral dimension of the tracer plume in the horizontal plane is very small.

Due to the unexpected high travel velocity of the plume, the initial plume behavior was not mapped in great detail because the sampling program was not appropriately designed at the test time. However, the subsequent tracer test with chloride gave data at the short distances with a modified sampling frequency. Data from this test can therefore in some ways supplement the missing information from the tritium test.

Figure 4 shows the concentration distribution in a vertical section placed along the longitudinal axis of the plume. The contouring is done on the basis of data projected onto the cross section from the measurement positions located at or nearby the longitudinal axis. A rather small vertical spreading is observed. Note that no downward movement of the plume takes place, indicating that the migration is not affected by density contrasts. In fact, on the contrary, the center of mass seems to move a little upward, as is indicated in the second graph. It is unlikely that this behavior is caused by evaporation from the water table and we believe it to be caused by local heterogeneities.

In Figure 5 breakthrough curves are displayed for the various levels at selected positions along the longitudinal axis. Most of the curves are in the shape of a Gaussian distribution, although some of the responses at the most downstream locations have a bimodal shape. This appearance is probably caused by a slight difference in the trajectories taken by different parts of the plume. The curves display several properties that could be anticipated such as a gradual broadening of the breakthroughs and decreasing

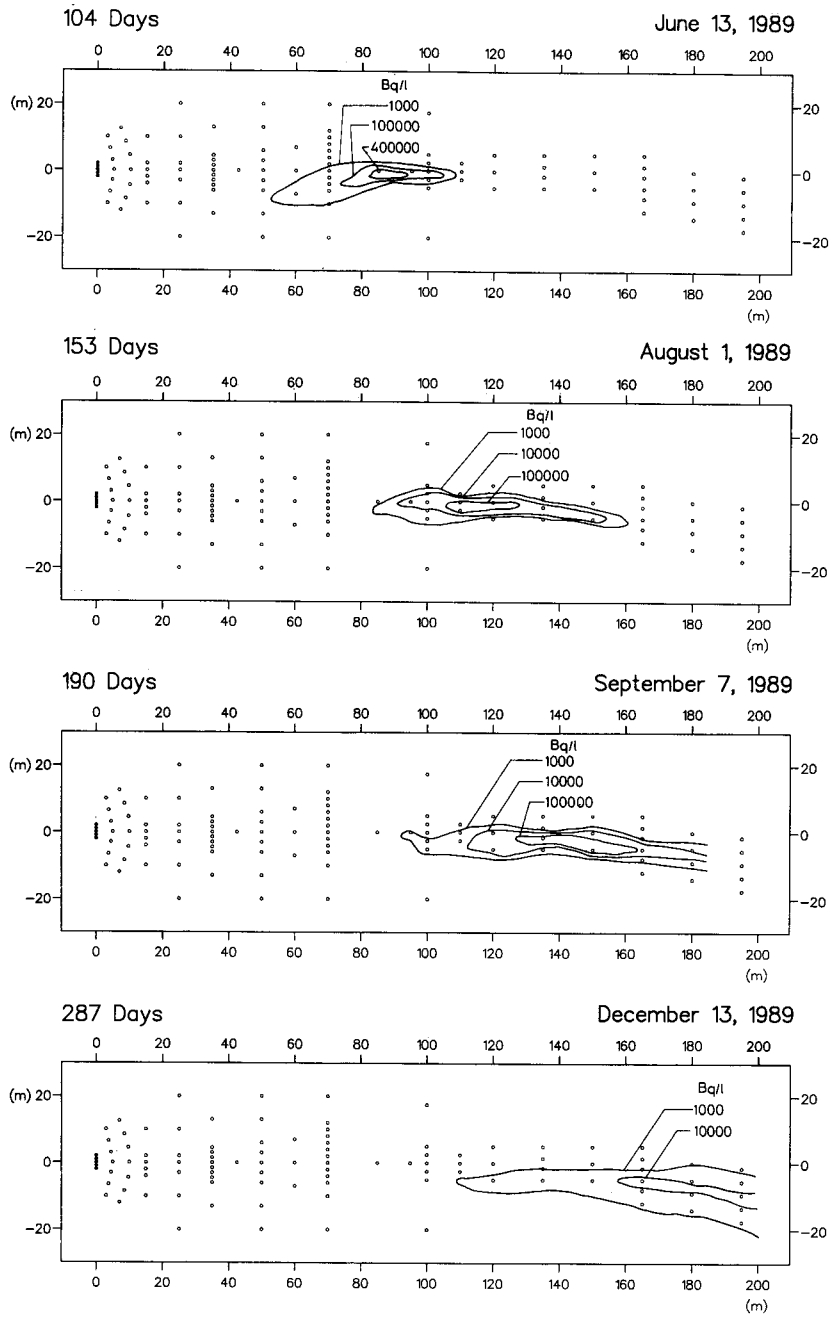

Fig. 3. Horizontal distribution of "vertically averaged" tritium concentrations.

peaks. It is also evident that the tracer tends to concentrate around a very few measuring locations.

4.2. *Chloride*

The horizontal movement of chloride (vertical averaging procedure as for tritium) shown in Figure 6 behaved in many ways similar to the tritium plume. The ratio of the longitudinal dimension to the lateral dimension is of the same order as for the tritium plume, although the chloride plume tends to be a little wider due to the sinking of the plume and the influence of the impermeable clay layer. The slope of the clay layer in transverse direction also gives rise to the splitting of the 500-mg/L concentration region. The horizontal velocity of the chloride plume is approximately 0.7 m/d which is a little less than the velocity of the tritium plume.

The movement of the chloride plume in the vertical direction was completely different from the behavior observed in the first tracer experiment. As is shown in Figure 7, large concentrations are observed just above the clay layer, and the center of mass of chloride is found significantly below the level of injection. Note that the plume tends to maintain the same shape for travel distances up to 100 m.

Figure 8 illustrates breakthrough curves at different vertical sections from the injection location. This figure also clearly shows the downward movement of the plume observed to take place right after injection. Two mechanisms may be responsible for this behavior: (1) vertical velocity

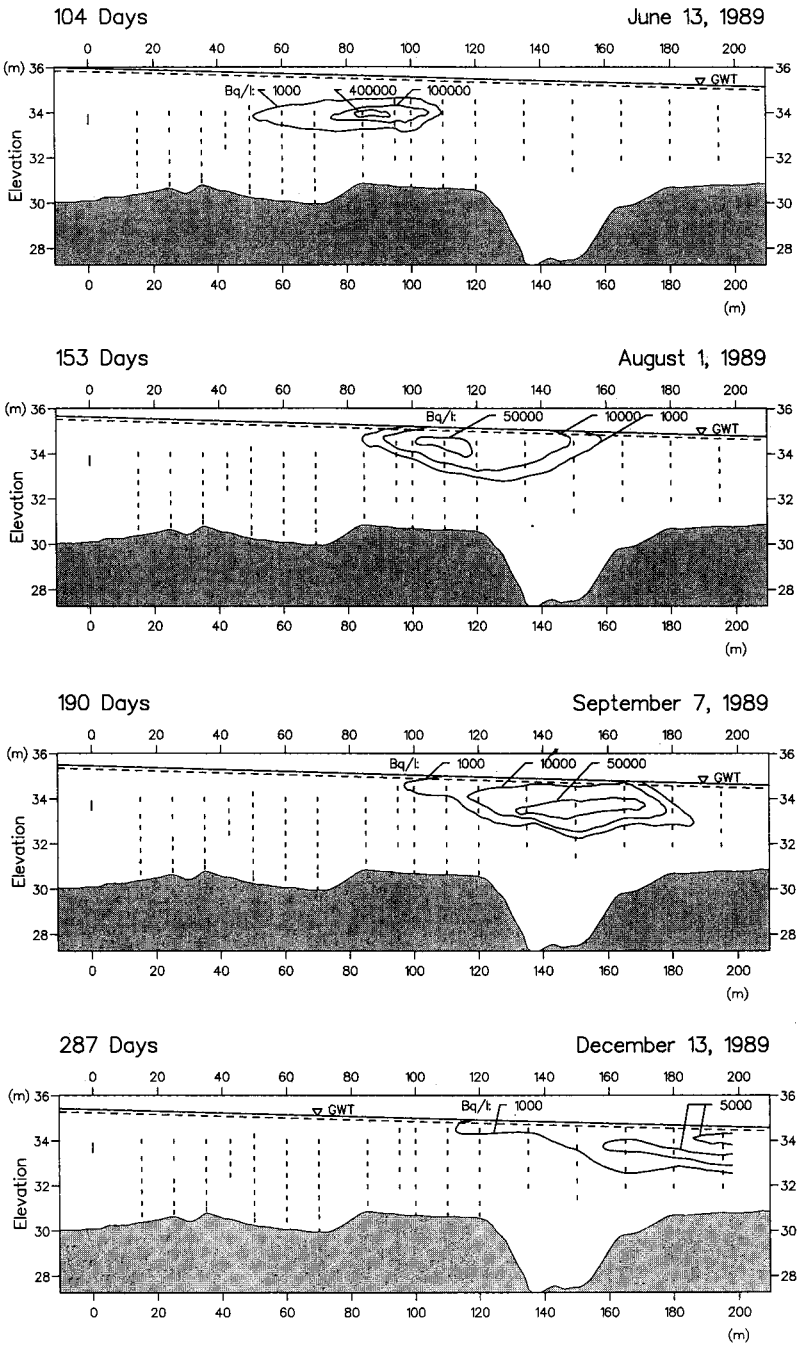

Fig. 4. Distribution of tritium concentrations in a vertical section along the longitudinal axis of the plume.

components caused by the driving head applied during injection and (2) density-driven transport. During the period of injection a driving head less than a few centimeters was created in the injection wells, so we attribute the vertical displacement to the density contrast between the injected fluid and the native groundwater. *Garabedian et al.* [1988] and *Freyberg* [1986] both reported a sinking due to density differences for contrasts much less than in the present case, and in a study by *Schincariol and Schwartz* [1990] the sinking of a denser fluid was clearly demonstrated for velocity and density conditions comparable to our case. They also observed the development of gravitational instabilities for large plume concentrations, a phenomenon which may contribute to enhanced spreading of solute perpendicular to the ambient flow direction.

5. Analysis of Dispersivity Parameters

We have analyzed the behavior of the dispersivity parameters on the basis of breakthrough curves by fitting an analytical solution of the advection-dispersion equation to the observed data. *Sudicky et al.* [1983] and *Moltyaner and Killey* [1988*a*, *b*] have used an analytical solution describing the migration of a tracer released as a rectangular parallelepiped, while others [e.g., *Leland and Hillel*, 1982] have applied the solution for the case of an instantaneous point

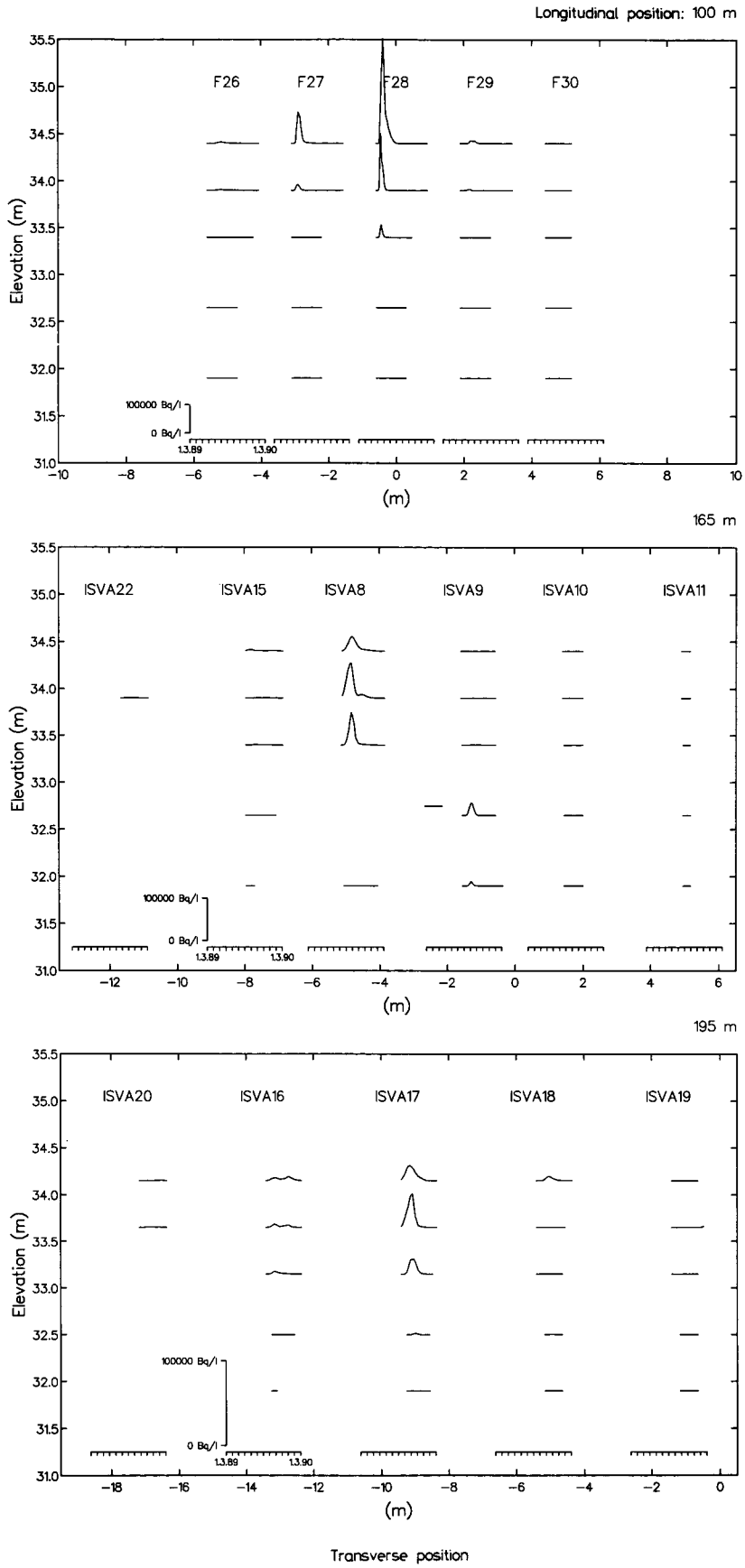

Fig. 5. Breakthrough curves of tritium in screens placed in vertical planes perpendicular to the longitudinal axis at different distances from injection wells.

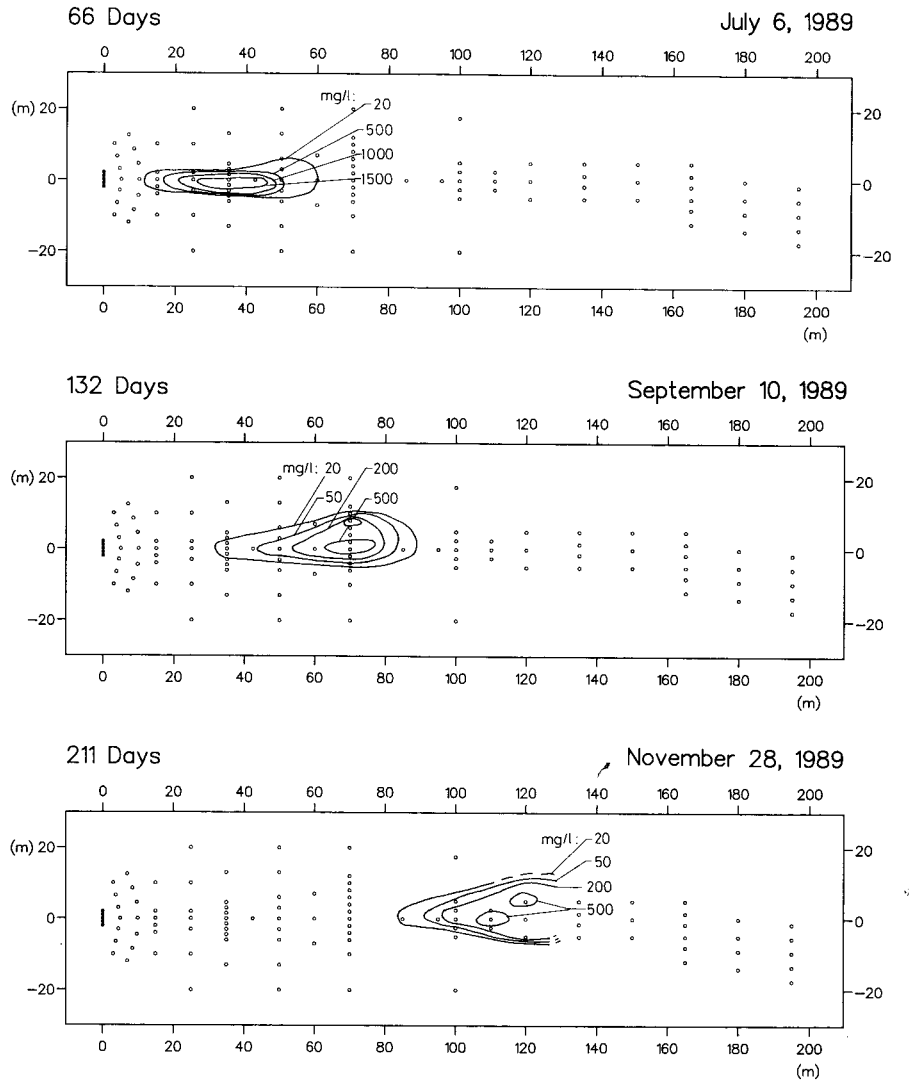

Fig. 6. Horizontal distribution of "vertically averaged" chloride concentrations.

injection. The following analysis is based on the latter approximation. All these analytical solutions are based on the assumption that the flow is unidirectional with a uniform velocity. Hence whatever analytical model applied will inevitably provide only an approximate description of the transport and dispersion processes taking place in the field. Thus the derived dispersivity parameters may therefore be considered as only approximate.

We have limited the analysis to the tritium test because the sinking of the chloride plume makes this experiment less suitable for simulation by an analytical model. In the following analysis we have focused on the horizontal components of the transport parameters because the vertical spreading of the tritium plume was rather small over the travel distances examined, and our main concern is to test for spatial trends in the horizontal components of seepage velocity and dispersivity. Hence the analysis is based on vertically averaged concentrations which essentially represent the total mass of tracer present in the vertical at a given horizontal location. A parameter identification model developed by *Sauty and Kinzelbach* [1988*a*, *b*] has been used to identify the transport parameters at a number of observation points in the horizontal direction. The model allows for optimization of flow velocity, flow direction, and longitudinal and transverse dispersivities in a horizontal two-dimensional uniform flow field.

For an instantaneous injection of a tracer slug in a horizontal two-dimensional, uniform flow field at the coordinate origin, the concentration distribution is described by [*Bear*, 1979]

$$C(x, y, t) = \frac{M}{4\pi nbt(D_{LH}D_{TH})^{0.5}} \cdot \exp\left(-\frac{(x-ut)^2}{4D_{LH}t} - \frac{y^2}{4D_{TH}t}\right) \quad (1)$$

where

C concentration;
M injection mass;
n porosity;
b aquifer thickness;
u flow velocity in x direction;
D_{LH} longitudinal horizontal dispersion coefficient;
D_{TH} transverse horizontal dispersion coefficient;
x, y horizontal space coordinates;
t time coordinate.

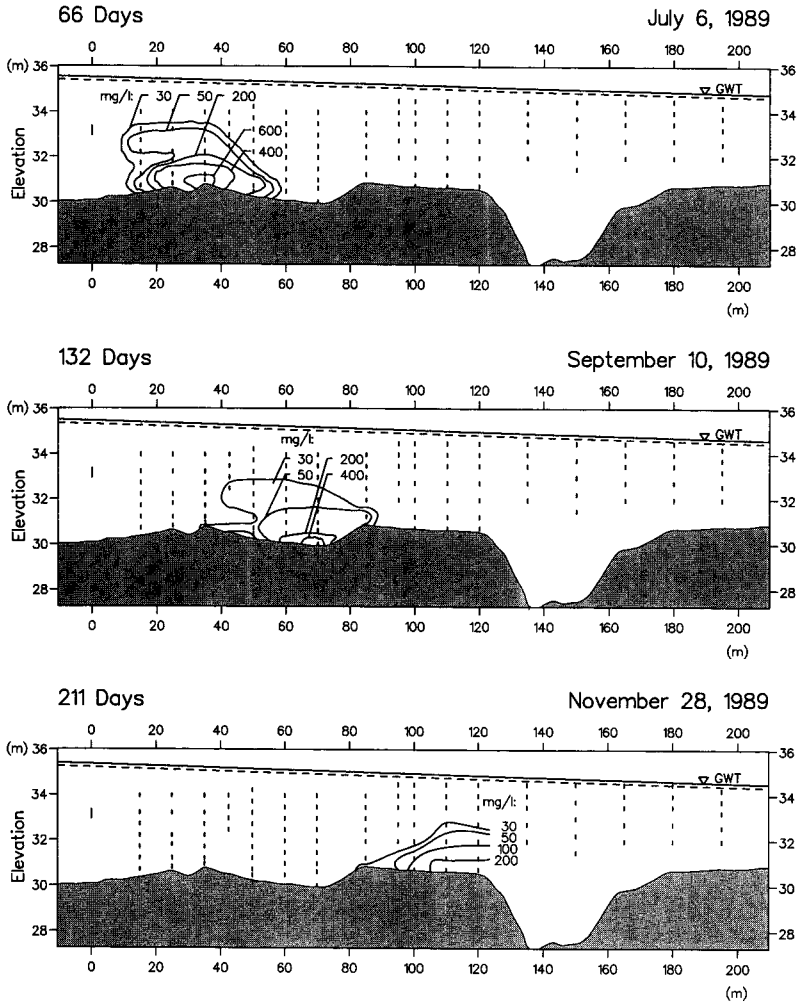

Fig. 7. Distribution of chloride concentrations in a vertical section along the longitudinal axis of the plume.

In this case, dispersion coefficients are related to the dispersivity coefficients by

$$D_{LH} = \alpha_{LH} u$$
$$D_{TH} = \alpha_{TH} u \tag{2}$$

where α_{LH} is longitudinal dispersivity and α_{TH} is transverse horizontal dispersivity.

The solution has been extended by *Sauty and Kinzelbach* [1988*a*, *b*] to an arbitrary direction of flow by introducing a coordinate transformation from the actual (x, y) to one oriented in the flow direction (x^*, y^*):

$$x^* = x \cos \theta + y \sin \theta$$
$$y^* = y \cos \theta - x \sin \theta \tag{3}$$

where θ is the angle between the direction of flow and the x axis.

Assuming that the vertically averaged tritium concentration data (normalized over a 0.5-m aquifer depth interval with a porosity of 0.30) can be described by this extended analytical equation, the transport parameters have been optimized in a two-step procedure using the sum of squares of the differences between measured and predicted concentrations as the objective function. First, the flow direction is determined for each row of piezometers placed perpendicularly to the longitudinal direction of the test field by including the measured average concentrations from all piezometers of the specific row in the optimization process. Second, the identified flow direction is kept fixed for the individual rows while flow velocity and dispersivities are optimized individually for all piezometers within a given row. The results are summarized in Table 2 for those piezometers where the complete breakthrough curves can be established from the measurements. Note that the lateral dispersivity will be overestimated using the present approach, because the injection source has a lateral dimension of 2 m, and this is not accounted for in the analytical model. However, the results are still valid for an initial parameter estimation and identification of spatial trends in the transport parameters. Figure 9 shows some typical matches to observed breakthrough curves indicating that it is possible to fit the analytical solution to the observations fairly closely.

As is indicated in Table 2, the transport parameters vary somewhat between the observation points, which is an indication of geological heterogeneity present in the aquifer not accounted for in the present rather simple analysis. However, the range of variation of all parameters is rather small. The optimized horizontal displacement velocity varies between 0.58 and 0.88 m/d with an average value of 0.75 m/d. The values listed in Table 2 suggest that the apparent

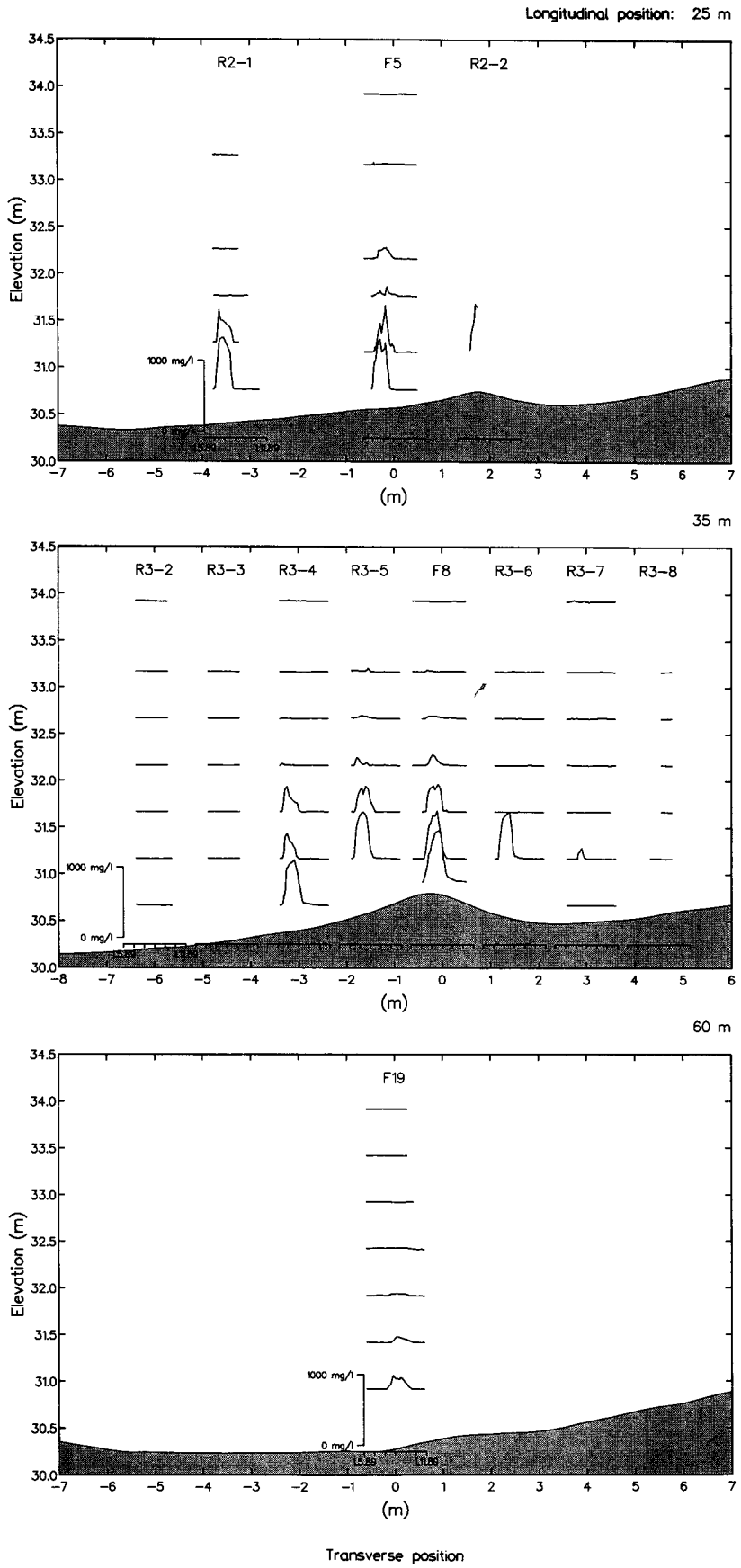

Fig. 8. Breakthrough curves of chloride in screens placed in vertical planes perpendicular to the longitudinal axis at different distances from injection wells.

TABLE 2. Optimized Transport Parameters

Observation Well	θ deg	u, m/d	α_{LH}, m	α_{TH}, m
f18	−1.35	0.63	0.42	0.056
f19	−1.35	0.88	0.52	0.065
f21	−0.21	0.62	0.13	0.076
f22	−0.21	0.88	0.57	0.007
f22*	−0.21	0.86	0.35	0.010
f24	0.0	0.84	0.13	0.013
f25	0.0	0.82	0.41	0.012
f26	−0.31	0.73	1.85	0.015
f26*	−0.31	0.68	0.45	0.014
f27	−0.31	0.83	0.26	0.068
f28	−0.31	0.86	0.32	0.004
f29	−0.31	0.73	0.55	0.007
f31	−1.17	0.78	0.27	0.038
f32	−1.17	0.77	0.49	0.023
f34	−0.79	0.60	0.83	0.009
f34*	−0.79	0.61	0.39	0.008
f35	−0.79	0.80	0.47	0.005
ISVA1	−0.85	0.70	1.99	0.006
ISVA1*	−0.85	0.79	0.20	0.004
ISVA2	−0.85	0.74	0.48	0.040
ISVA3	−0.85	0.66	0.20	0.003
ISVA5	−1.79	0.79	0.55	0.020
ISVA6	−1.79	0.78	0.29	0.019
ISVA8	−1.36	0.79	0.52	0.005
ISVA9	−1.36	0.76	0.18	0.004
ISVA12	−1.13	0.78	0.46	0.026
ISVA14	−1.13	0.77	1.40	0.026
ISVA14*	−1.13	0.81	0.48	0.018
ISVA15	−1.36	0.72	1.98	0.007
ISVA15*	−1.36	0.79	0.48	0.006
ISVA16	−2.8	0.78	1.99	0.009
ISVA16*	−2.8	0.82	0.40	0.007
ISVA17	−2.8	0.79	0.66	0.037
ISVA18	−2.8	0.76	0.43	0.006
ISVA19	−2.8	0.73	0.78	0.013
ISVA20	−2.8	0.68	0.70	0.024
ISVA21	−1.13	0.64	0.76	0.041
ISVA22	−1.36	0.58	0.44	0.028
Mean		0.75	0.42	0.023

Here θ is flow direction, u is convective horizontal velocity, α_{LH} is longitudinal horizontal dispersivity, and α_{TH} is transverse horizontal dispersivity.

*Manual fit, automatic fitting not successful.

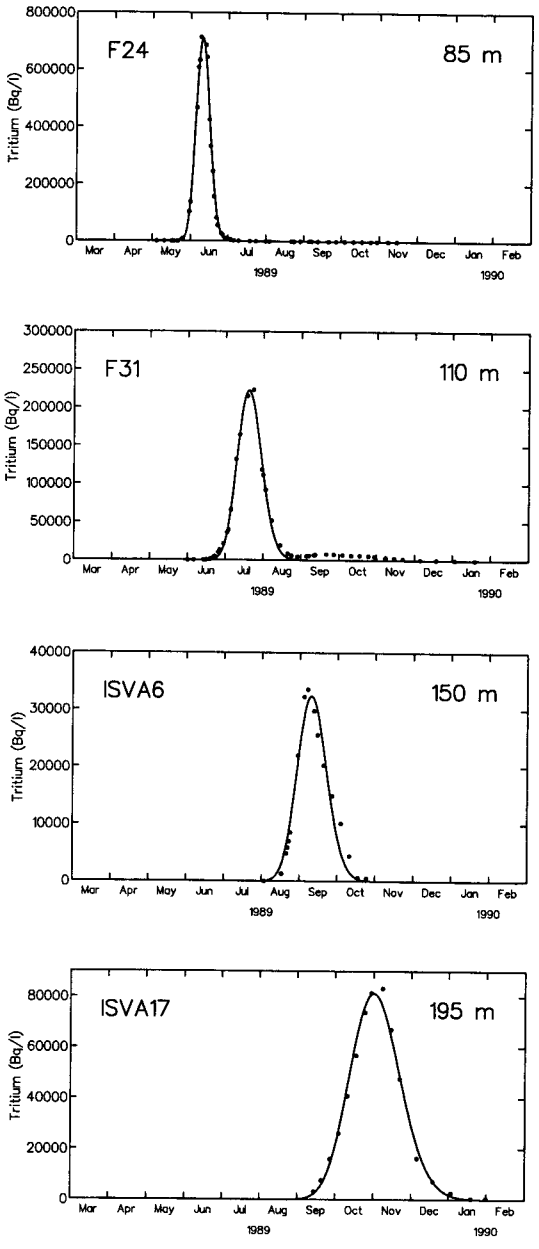

Fig. 9. Observed (dots) and fitted (lines) breakthrough curves of vertically averaged tritium concentrations.

velocity is slightly above the average value in the upstream end and slightly below average further downstream.

For the longitudinal and transverse horizontal dispersivities no clear trend with travel distance can be found contrary to the tests reported by *Freyberg* [1986] and *Garabedian et al.* [1991]. The optimized values for the locations listed in Table 2 vary more or less arbitrarily around the mean values of 0.42 and 0.02 m for the longitudinal and transverse dispersivity, respectively, thus indicating that the asymptotic stage of the development of the dispersivity parameter had been reached for the distances examined. The variation appearing in Table 2 can be explained by the aquifer heterogeneity, which then gives rise to different dispersivities, because the actual flow trajectories are not included in the analysis.

The dispersivities obtained in this analysis seem rather small for this particular scale of transport distance when compared to values reported elsewhere [e.g., *Gelhar et al.*, 1985] and the values often applied in engineering practice. Yet they are consistent with the magnitudes obtained in the Borden and Cape Cod cases.

Although small values are obtained for the dispersivities, they may in reality be somewhat overestimated due to the parameter identification method. Actual velocity variations over the aquifer thickness may be reflected by enhanced longitudinal dispersivities calculated, because this analysis is based on vertically averaged concentrations. Also, seasonal fluctuations in the flow regime as well as the initial lateral dimension of the injected tracer source may introduce an additional artificial increase in the calculated dispersivities. Later we apply a three-dimensional numerical model which provides a more realistic description of the actual field conditions in order to appraise the parameters found by the present rather simplified analysis.

Gelhar and Axness [1983] have developed theoretical expressions for the macroscopic dispersivity tensor. Of particular interest are the asymptotic values which for the two-dimensional case are given by

$$A_{11} = \sigma^2_{\ln K}\lambda_{\ln K}$$
$$A_{22} = \sigma^2_{\ln K}(\alpha_1 + 3\alpha_2)/8 \quad (4)$$

where $\sigma^2_{\ln K}$ represents the variance of the logarithmic transformed hydraulic conductivity, $\lambda_{\ln K}$ is the correlation length, and α_1 and α_2 are the local dispersivities.

Using the data on the correlation structure of the hydraulic conductivity field ($\sigma^2_{\ln K} = 0.37$, $\lambda_{\ln K} \approx 1.5$ m) and assuming that the local dispersivities are of the order of a millimeter ($\alpha_1 = 0.005$ m, $\alpha_2 = 0.0005$ m), the theoretically derived asymptotic macrodispersivities are

$$A_{11} = 0.55 \text{ m}$$
$$A_{22} = 3 \times 10^{-4} \text{ m}$$

The longitudinal dispersivity conforms rather closely to the average value listed in Table 2, while the theoretical value for the transverse dispersivity is much smaller. However, as is described above, the average transverse dispersivity given in Table 2 is estimated too high and, in fact, the theoretical value is not very far from the value calculated in the numerical analysis discussed below.

The hypothesized increase in dispersivity with travel distance has not been examined, because we are not able to recover reliable breakthrough data for the initial phase of the experiment with tritium. The analysis suggests that the asymptotic value of dispersivity is already reached at the smallest distance (50 m) for which complete breakthrough data are available. This observation agrees with the theoretically derived expressions for the development of longitudinal dispersivity with displacement distance, according to which the asymptotic stage is reached after approximately 10 correlation lengths [*Gelhar and Axness*, 1983].

The ideal method for analyzing the transport and dispersion characteristics of a tracer experiment is a spatial moment analysis, where the moments define integrated measures of total mass, mean velocity, and dispersion of the plume. Moments are estimated on the basis of point observations using some numerical integration techniques. The moment analysis method has been successfully used both in the Borden and Cape Cod experiments as described by *Freyberg* [1986] and *Garabedian et al.* [1991], respectively. Application of this method requires a very dense sampling network in order to accurately derive the moments. Although the present field test also includes a large number of observation points, it is not as dense as for the two other sites. Due to the limited extent of the plume, the "snapshots" of three-dimensional spatial distribution of the tracer concentration at particular times are not very accurately defined because only a relatively small number of observation wells are affected, and hence it is not feasible to apply this technique in our study.

6. Numerical Simulations of Flow and Tracer Transport

6.1. *Numerical Model*

A three-dimensional numerical model with a fine discretization has been applied to accurately simulate the movement of the tracer plumes. Using a numerical model it is possible to incorporate all the data collected on the geological stratification and the hydraulic conductivity distribution and to consider the seasonal fluctuations of recharge and the concentration data.

We have applied the three-dimensional finite difference groundwater flow and transport model developed as part of the European Hydrological System (SHE) [*Danish Hydraulic Institute*, 1992].

The flow description of the model is based on the governing equation for three-dimensional Darcian groundwater [e.g., *Freeze and Cherry*, 1979]. In the numerical formulation this equation is approximated by a set of coupled algebraic equations which are obtained by applying Darcy's law and the water balance equation in finite difference forms to each node in the solution domain assuming that flow occurs in directions between the specific node and its six direct neighbor nodes. The equations are formulated in an implicit scheme where the internode hydraulic conductivity is obtained as the harmonic mean. The system of linear finite equations is solved for hydraulic head in a modified Gauss-Seidel iterative scheme [*Thomas*, 1973].

The transport of solutes in constant density groundwater is described by the three-dimensional advection-dispersion equation [e.g., *Freeze and Cherry*, 1979], where the dispersion coefficient is related to the groundwater flow velocity using *Scheidegger*'s [1961] relationship, which in tensor notation reads

$$D_{ij} = \alpha_{ijmn}\frac{u_m u_n}{|u|} \qquad i, j, m, n = 1, 2, 3 \quad (5)$$

where α is dispersivity, u is seepage velocity, and $|u|$ is magnitude of seepage velocity. In the general three-dimensional case of arbitrary flow direction in an anisotropic aquifer the dispersion tensor contains 9 components which depend on a dispersivity tensor containing 81 components; symmetry properties reduce the number of components to 36. A further simplification is obtained if cubic symmetry is assumed in which case the number of components is reduced to 12 [*Scheidegger*, 1961].

In the present case the groundwater flow direction is aligned rather closely with the orientation of the x axis of the coordinate system which is placed along the longitudinal axis of the test field site. Under these circumstances it seems justified to neglect the off-diagonal terms of the dispersion tensor, which simplifies the numerical computations significantly and hence the computational burden. Thus only the D_{11}, D_{22}, and D_{33} components will be accounted for in the numerical solution.

The components of the dispersivity tensor entering the diagonal components of the dispersion tensor can be grouped into the following four physically recognizable parameters: α_{LH} (longitudinal horizontal dispersivity); α_{TH} (transverse horizontal dispersivity); α_{LV} (longitudinal vertical dispersivity); and α_{TV} (transverse vertical dispersivity).

Hence we obtain the following expressions for the diagonal terms:

$$D_{11} = \alpha_{LH}\frac{u_1u_1}{|u|} + \alpha_{TH}\frac{u_2u_2}{|u|} + \alpha_{TV}\frac{u_3u_3}{|u|}$$
$$D_{22} = \alpha_{TH}\frac{u_1u_1}{|u|} + \alpha_{LH}\frac{u_2u_2}{|u|} + \alpha_{TV}\frac{u_3u_3}{|u|} \quad (6)$$
$$D_{33} = \alpha_{TV}\frac{u_1u_1}{|u|} + \alpha_{TV}\frac{u_2u_2}{|u|} + \alpha_{LV}\frac{u_3u_3}{|u|}$$

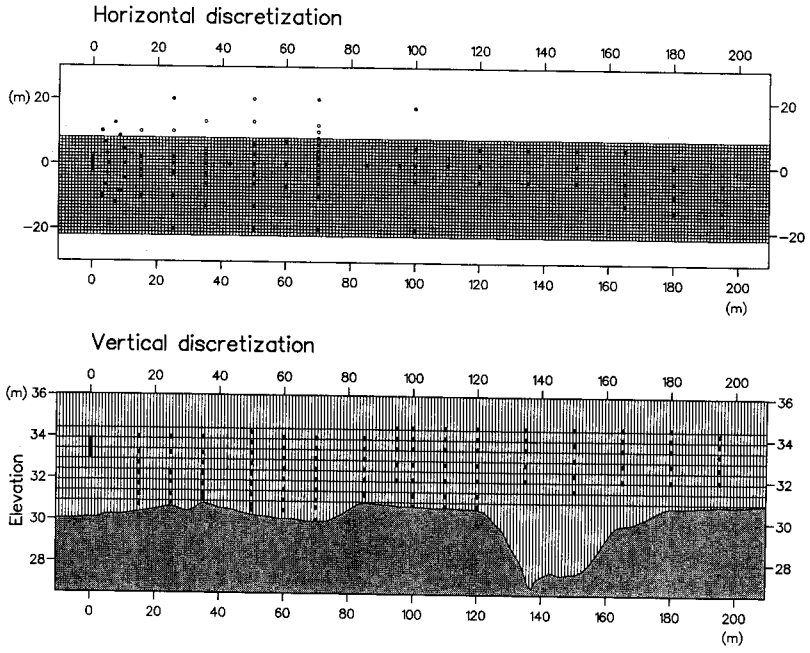

Fig. 10. Horizontal and vertical grid spacing in numerical model.

Under these assumptions the SHE solves the advection-dispersion equation by finite difference techniques using an explicit third-order accurate interpolation scheme as described by *Vested et al.* [1992]. This scheme is mass conservative and enables simulation of sharp advective fronts without smearing from numerical dispersion. Due to the explicit formulation the time step is constrained by requirements to maximum allowable advective and dispersive transport distances.

6.2. *Model Application*

The affected part of the aquifer has been divided into a large number of cells to form the finite difference grid. The horizontal grid spacing is 1.0 m, while the vertical spacing is 0.5 m in the region traversed by the plumes and variable at the top and bottom of the model region. This results in 220 × 30 nodes in the horizontal and 9 in the vertical for a total of 59,400 nodes used for the computations (Figure 10). The numerical discretization has been defined as a compromise between high spatial resolution and computer simulation time.

The upper boundary condition in the form of recharge to the water table was generated by applying a one-dimensional unsaturated flow and evapotranspiration model developed by *Jensen* [1983]. On the basis of daily observations of rainfall and potential evapotranspiration and site-specific soil hydraulic properties, the model predicts the water flux across the water table which constitutes inflow to the groundwater model.

The boundary conditions along the vertical planes which form the sides to the model region in the horizontal directions are prescribed hydraulic heads assuming that hydrostatic conditions apply. The fluctuations in hydraulic heads along the model boundary were generated by applying the two-dimensional flow model of the U.S. Geological Survey's method of characteristics code [*Konikow and Bredehoeft*, 1978] to the regional aquifer containing the experimental site. The boundaries of the regional model are placed along creeks when possible and otherwise far away from the area of interest. The fluctuations in recharge for the regional model were also predicted by the unsaturated flow model [*Jensen*, 1983].

The lower confinement of the model is provided by the layer of low-permeable silt/clay sediments (Figure 10).

The time steps used in the numerical model are variable: of the order of 7 days for the flow and 7 hours for the transport computations.

6.3. *Simulation Results (Homogeneous Three-Layer Model)*

The first series of model simulations are based on the assumption that the aquifer is composed of three homogeneous layers. The hydraulic conductivity values (K_g) and the thicknesses of the individual layers are listed in Table 1. The upper and lower layers are extended to the top and the bottom of the model region, respectively. Since the aquifer is composed of alluvial deposits, the vertical hydraulic conductivity is smaller than the horizontal one. On the basis of calibration and past experiences with the particular geologic environment we have estimated the anisotropy factor to 50. This value is larger than predicted by the *Gelhar and Axness* [1983] theory; however, it is consistent with the factor applied in a large-scale model study in the same area [*Jensen et al.*, 1991]. In any case, the vertical hydraulic conductivity has only little influence on the model simulations due to the small vertical velocity components. For the specific storage coefficient or drainable porosity a value of 0.20 is specified in the upper discretization blocks containing the water table (unconfined conditions), while a value of 0.001 is applied in blocks where the hydraulic head level is above the level of the upper confinement (artesian conditions). For the kinematic porosity a value of 0.30 is assumed. All the simulation results presented below are based on transient flow conditions.

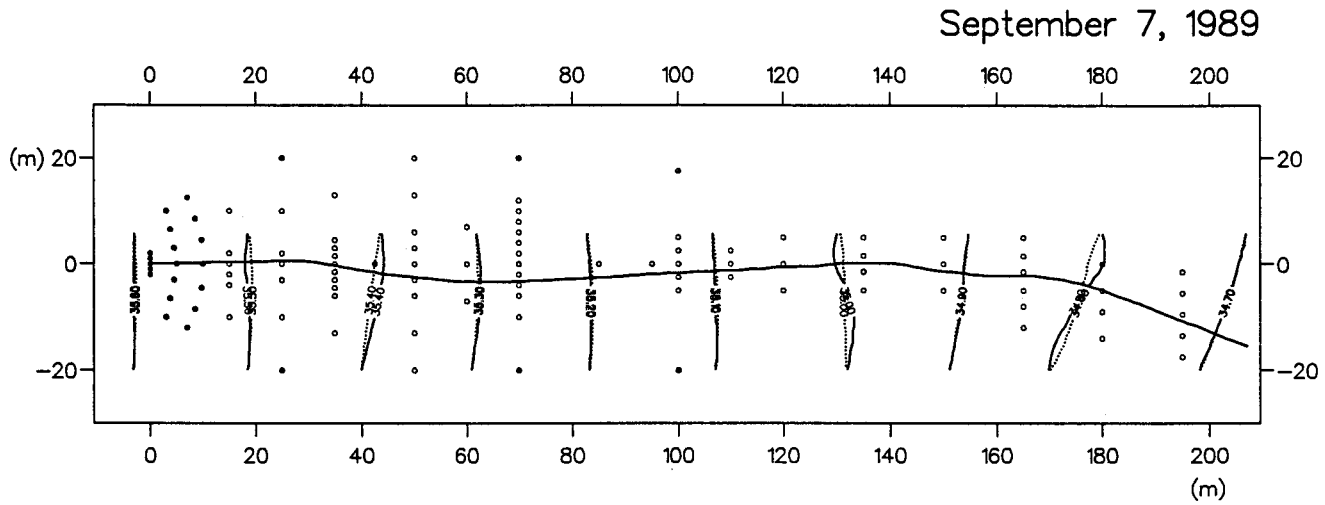

Fig. 11. Observed (dotted lines) and simulated (solid lines) water table configuration and flow trajectory.

On the basis of the rather simplified geometry of the aquifer and the boundary conditions discussed above, very accurate simulations of the water table configuration (Figure 11) as well as of the seasonal fluctuations (Figure 12) are obtained.

For the transport simulations of tritium we applied in the first attempt the values for the horizontal dispersivities found by the simplified analytical analysis discussed above. However, as anticipated, this resulted in a much more pronounced transverse spreading than observed, while the longitudinal component compared reasonably to the observations. A sensitivity analysis was subsequently carried out in order to identify the values for the dispersivities which gave the best match to the observed concentrations.

On the basis of this sensitivity analysis we identified the following best fit parameters: $\alpha_{LH} = 0.45$ m, $\alpha_{TH} = 0.001$ m, $\alpha_{LV} = 0.05$ m, and $\alpha_{TV} = 0.0005$ m. It should be emphasized that these parameters were not determined by a stringent optimization process but on the basis of a number of trial simulations.

The simulation results were sensitive to all parameters except the longitudinal vertical dispersivity α_{LV} because of small vertical flow components. Hence it was not possible to identify this parameter very accurately on the basis of the present experiment, and the value used in the simulations (0.05 m) was chosen on the basis of previous experiences with the model [e.g., *Jensen et al.*, 1991].

The best fit value for the longitudinal horizontal dispersivity α_{LH} conforms closely to the results of the previous analysis, while the transverse horizontal dispersivity α_{TH} had to be assigned a very low value in order to match the observed spreading. In relation to the previous analytical analysis, α_{TH} was reduced by one order of magnitude, partly because the lateral dimension of the injection was now taken into account, but also due to the fact that the spatial and temporal variations in the flow field were considered in the numerical model. The value for α_{TH} suggested in this study is lower than found in the Borden and Cape Cod cases.

Similarly, for the transverse vertical dispersivity α_{TV} an extremely low value (0.0005 m) was required in order to match simulations and observations. Also, for this parameter we observed a significant sensitivity of the simulation results and a value which essentially represents only molecular diffusion needed to be used in order to reproduce the steep concentration gradients observed. This finding is consistent with the results by *Frind et al.* [1989].

The simulation results based on the above values for the dispersivity parameters are shown in Figures 13, 14, and 15.

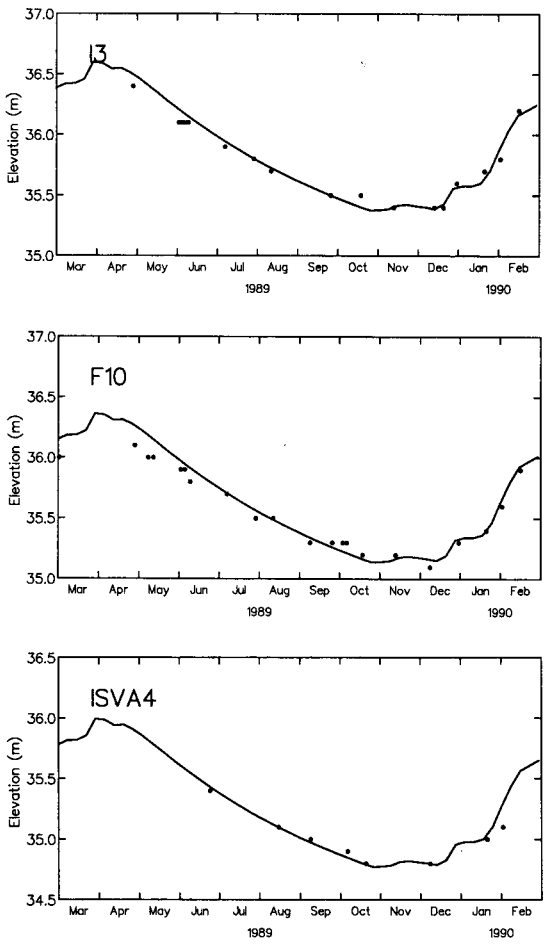

Fig. 12. Observed (dots) and simulated (lines) water table fluctuations in selected piezometers.

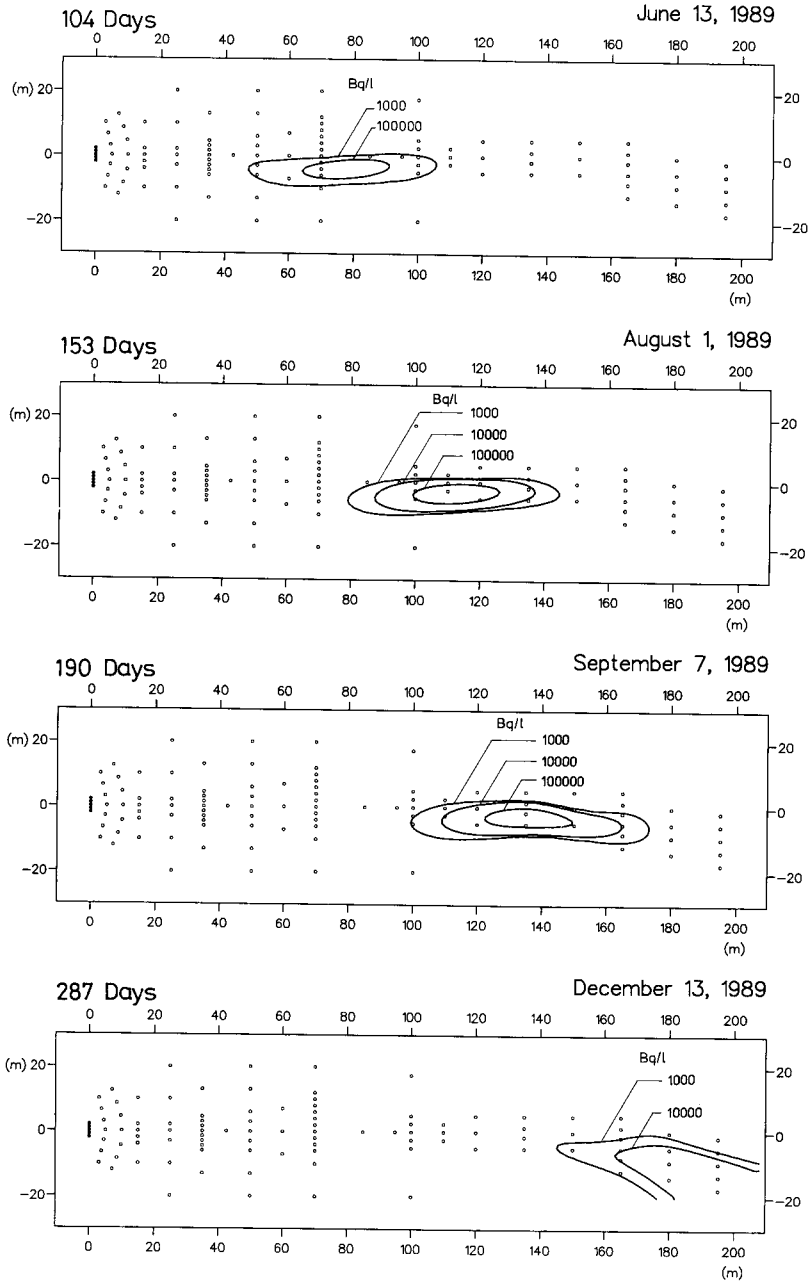

Fig. 13. Simulated horizontal distribution of "vertically averaged" tritium concentrations (homogeneous three-layer model).

Figure 13 presents contour plots of the vertically averaged tritium concentration at various times after injection, and Figure 14 shows concentration distributions of the tritium plume in vertical sections on the longitudinal axis of the plume at the same times. Figures 13 and 14 provide an overview of the overall behavior of the simulated tritium plume and by comparing to the observed behavior shown in Figures 3 and 4 it is seen that there is a good agreement as far as travel velocity and spreading in horizontal and vertical directions are concerned.

When compared on a more detailed scale as observed and simulated breakthrough curves, as exemplified in Figure 15, the discrepancies between the observed data and the numerical results become more apparent. In general, the simulated breakthrough curves mirror the shapes of the observed ones with respect to arrival times, base lengths on the time axis, and peak concentrations, although the spatial locations of the breakthroughs laterally as well as vertically within the cross sections displayed are not in exact agreement. We attribute the discrepancies shown by Figure 15 to the presence of local small-scale intraformational heterogeneities not accounted for in the hydraulic conductivity distribution used in the model. Such heterogeneities will locally influence the concentration distribution; however, the effects seem to average out on a larger scale. It is an impossible task to map the three-dimensional spatial distribution of the hydraulic properties at the scale of the mesh and, consequently, we cannot expect the model to be able to provide a complete resolution of the concentration variation observed at the individual point locations within the aquifer traversed by the

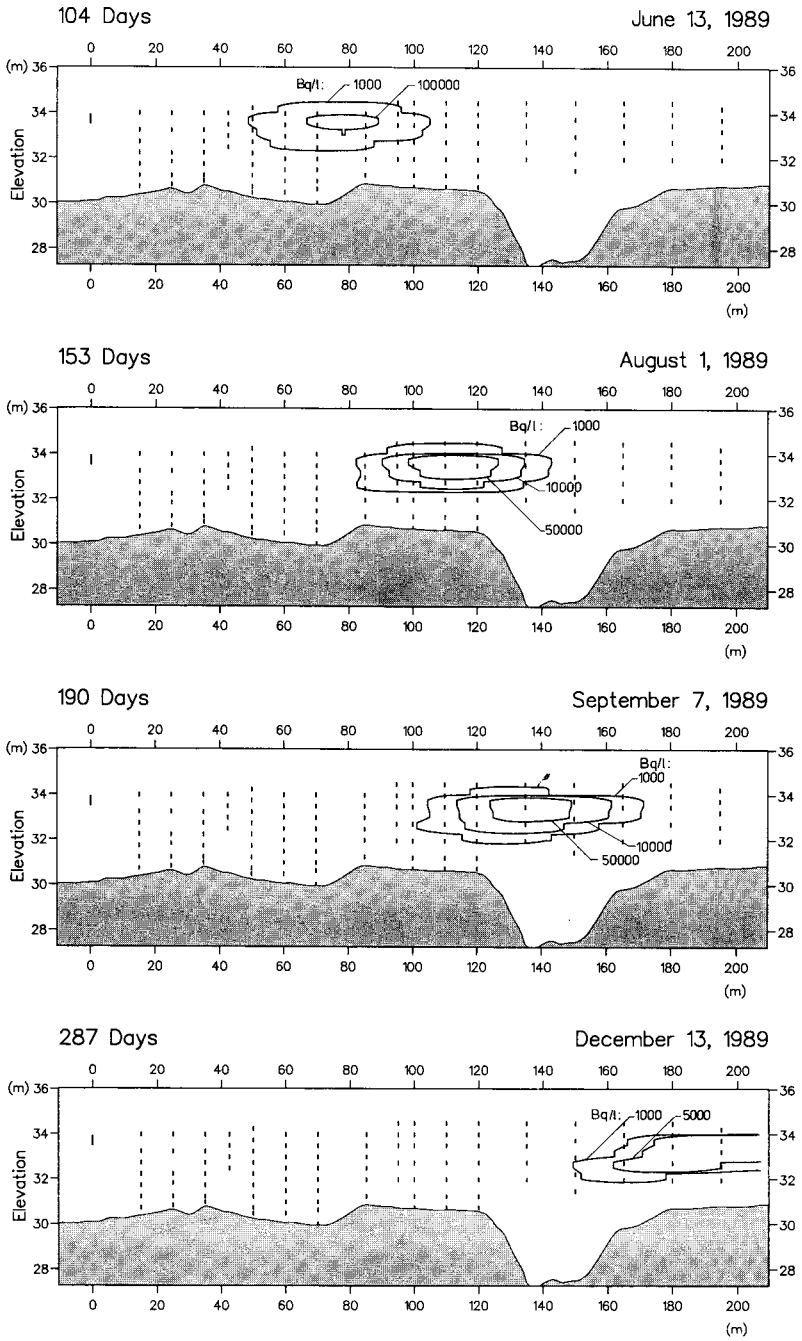

Fig. 14. Simulated vertical distribution of tritium (homogeneous three-layer model).

tracer. However, on an overall basis the model has reproduced the characteristics of the observed tracer distribution. The results suggest that dispersivities of magnitudes much smaller than reported by, for example, *Gelhar et al.* [1985] can be applied to field problems in alluvial aquifers if the overall structure of the sedimentary layers is defined.

The second tracer test involving chloride suffers from the problem of initial vertical displacement of the plume due to density contrasts between the tracer solution and the native groundwater. While the head effect can be accounted for in the numerical model it is not capable of describing the spreading produced by the presence of the higher-density tracer solution over the lower-density native groundwater.

As discussed previously, the density-driven vertical displacement of the solute plume takes place immediately below the injection point, leading to high concentrations just above the less-permeable clay layer. Furthermore, the experimental data indicate that the vertical shape of the plume remains essentially unchanged over the duration of the experiment (see Figure 7). In order to account for the initial density driven displacement in the numerical model we have empirically adjusted the injection source term by injecting the tracer solution over the vertical in proportion to the peak concentrations observed over the vertical 15 m downstream of the injection point.

Using the same dispersivity parameters as for the tritium

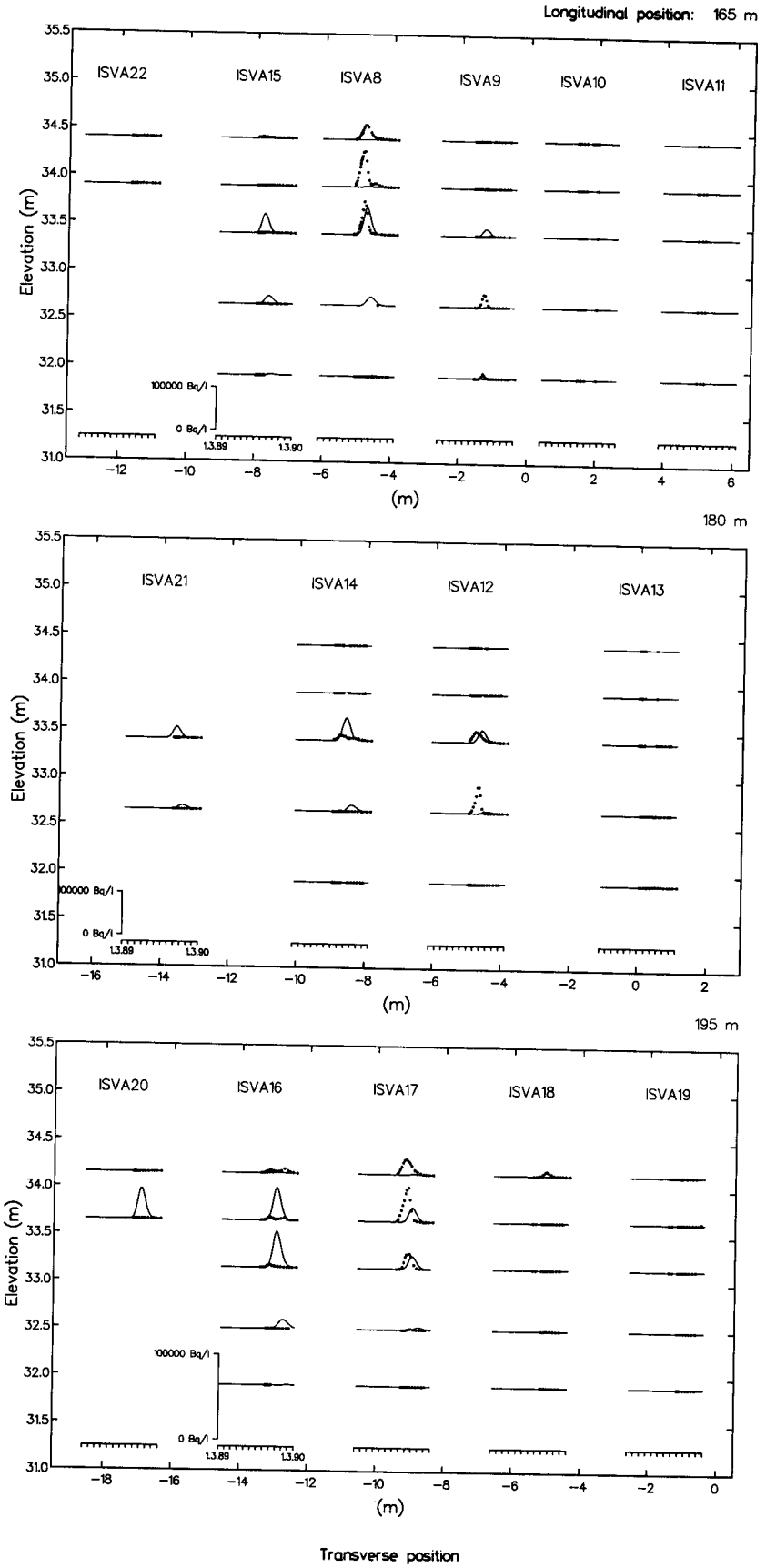

Fig. 15. Observed (dots) and simulated (lines) breakthrough curves of tritium (homogeneous three-layer model).

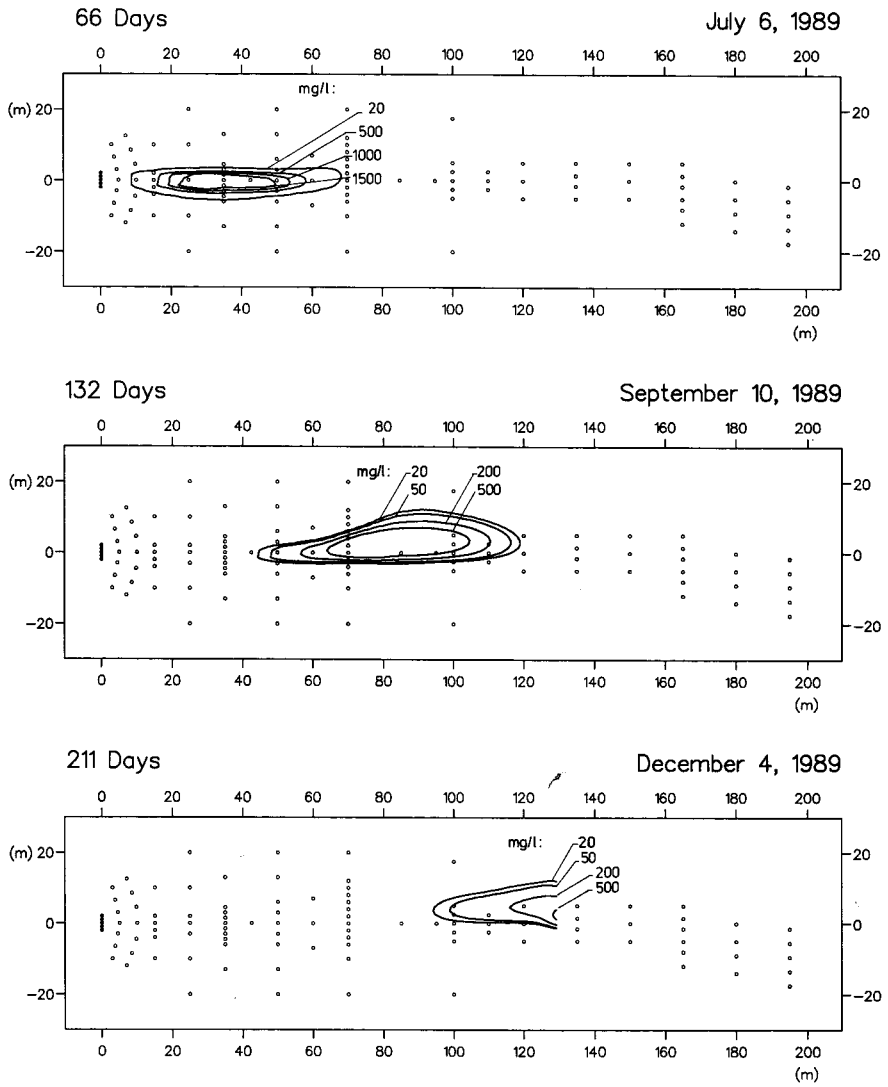

Fig. 16. Simulated horizontal distribution of "vertically averaged" chloride concentrations (homogeneous three-layer model).

simulations, the predictions of the movement of the chloride plume are shown in Figures 16–18. By comparing the simulation results to the observations presented in Figures 6 and 7 it is seen that both the horizontal and vertical shapes of the simulated plume compare rather well to the configurations observed. Also, the predicted horizontal displacement velocity compares favorably to the observed characteristics during the initial phase of the experiment (up to a travel distance of about 60 m); however, in the later phase the displacement velocity is somewhat overestimated.

Figure 18 compares predicted and observed breakthrough curves at various positions in cross sections placed in the near field. As is shown by the figure, an excellent agreement is obtained for the travel distances shown. For longer distances the times of arrivals are slightly offset, yet the shapes of the curves are still in good agreement. Hence the chloride data have confirmed the best fit dispersivity parameters obtained from the tritium simulation. This suggests that these parameters are also valid in the lower part of the aquifer.

6.4. *Simulation Results (Heterogeneous Three-Layer Model)*

The numerical model analysis discussed in section 6.3 was based on the assumption that the aquifer under investigation is composed of three structural sand layers each with uniform hydraulic properties. For the transport distances examined, the simulation of the plume movements based on this rather simple conceptualization of the geological composition was in good agreement with the experimental data for small values of the dispersivity tensor. However, the analysis also suggested that the concentration observations locally are influenced by small-scale intraformational heterogeneities which were not included in the numerical model.

In order to investigate the influence of the small-scale local variations in the hydraulic conductivity K on contaminant transport, that parameter was treated as a random variable. The relevant statistical parameters for characterizing the spatial variation of the hydraulic conductivity include the mean, the standard deviation, and the covariance.

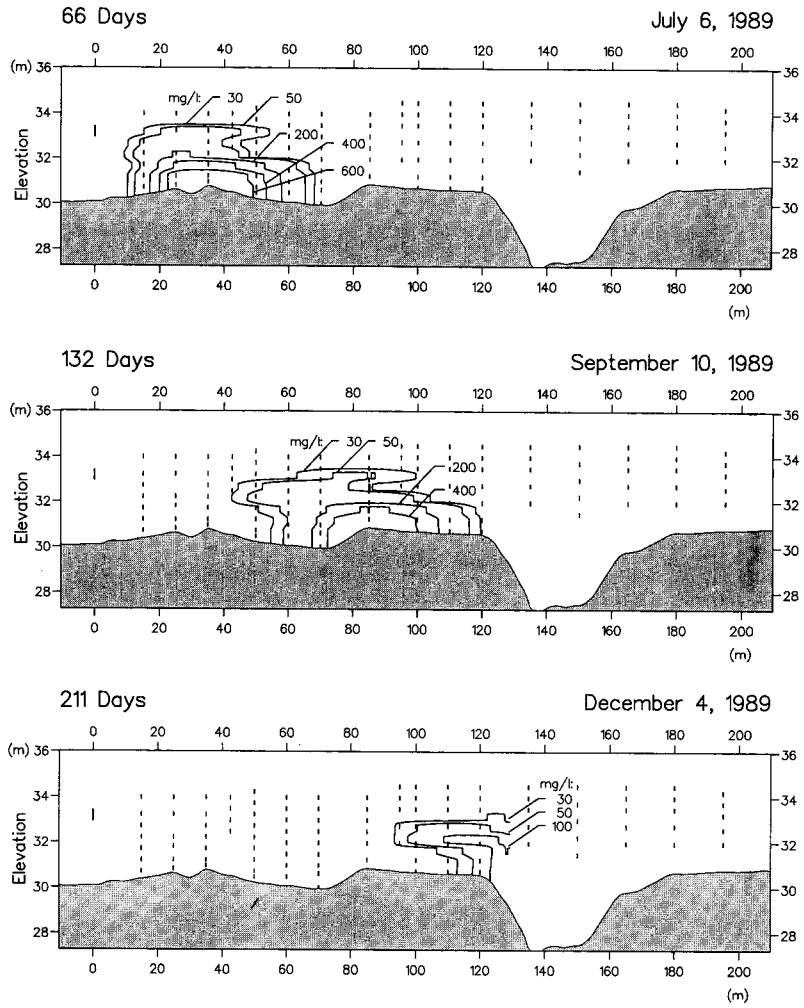

Fig. 17. Simulated vertical distribution of chloride (homogeneous three-layer model).

Due to excessive computational requirements of the three-dimensional flow and transport model it was not feasible to perform a traditional Monte Carlo analysis involving simulations for a large number of realizations of K. Instead, we have only analyzed the movement of the tracer plume under a single porous media realization.

Because of the large transport distance of the plume in comparison with the horizontal correlation scale of the hydraulic conductivity field, it was assumed that the transport characteristics of the simulated plume represented the ensemble average. The same approach has been used by *Ababou et al.* [1988] and *Sudicky et al.* [1990].

In order to generate random three-dimensional hydraulic conductivity fields with prescribed statistical properties the turning band method developed by *Mantoglou and Wilson* [1982] was used. It was assumed that the aquifer is composed of three statistically independent sedimentary layers with the statistical properties (mean, variance, and correlation length) listed in Table 1. Further, it was assumed that the spatial correlation structure of the log-transformed horizontal hydraulic conductivity spatial fluctuations could be described by an exponentially decaying function. No data were available for the correlation length in the vertical direction and therefore we estimated this parameter to be 0.15 m on the basis of a comparative analysis to the structural data given by *Sudicky* [1986] and *Hess et al.* [1991].

The computer code developed by *Tompson et al.* [1987] was used to generate a realization of the hydraulic conductivity fields with the statistical properties described above. Point values of hydraulic conductivity were generated on a grid with 1.0 m spacing in the horizontal direction and 0.10 m in the vertical. The vertical discretization was decreased relative to the homogeneous case in an attempt to preserve the statistical properties of the ln K field. The random field was not conditioned at the measurement locations, because of the small number of measurements present (250) in relation to the total number of grid elements involved (244,000) and the small correlation lengths of the hydraulic conductivity fluctuations. According to, e.g., *Ababou et al.* [1988] this grid may still be too coarse to accurately preserve the statistical properties in both directions. However, we had to compromise on the grid refinement in order to overcome the computer limitations; yet, we believe that the adopted grid is valid for providing an approximate estimate of the reduction in the dispersion parameter.

The single realization of the hydraulic conductivity field served as input to the numerical model, and for this particular case the flow field was assumed to be time invariant. In the first simulation the same dispersivity parameters as for

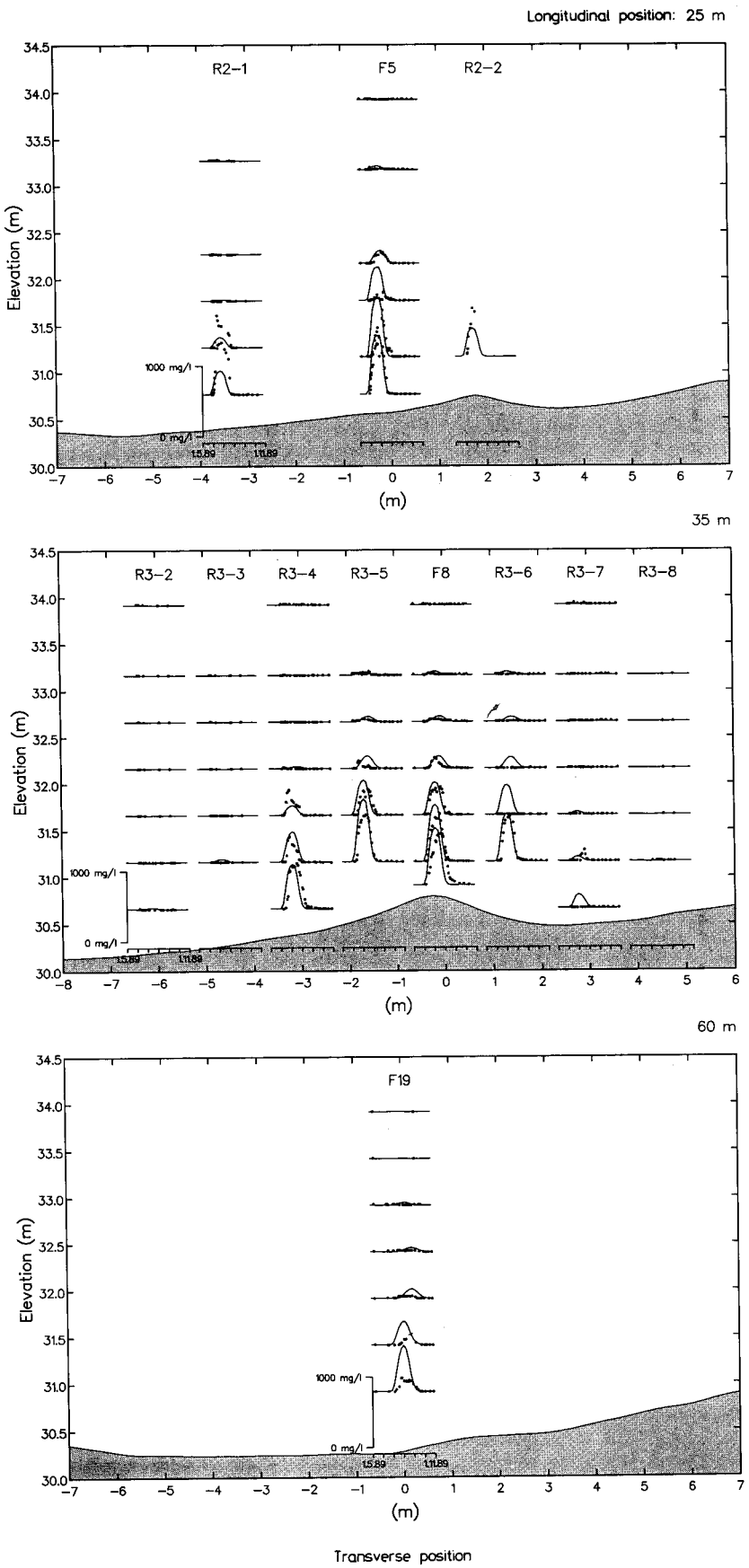

Fig. 18. Observed (dots) and simulated (solid lines) breakthrough curves of chloride (homogeneous three-layer model).

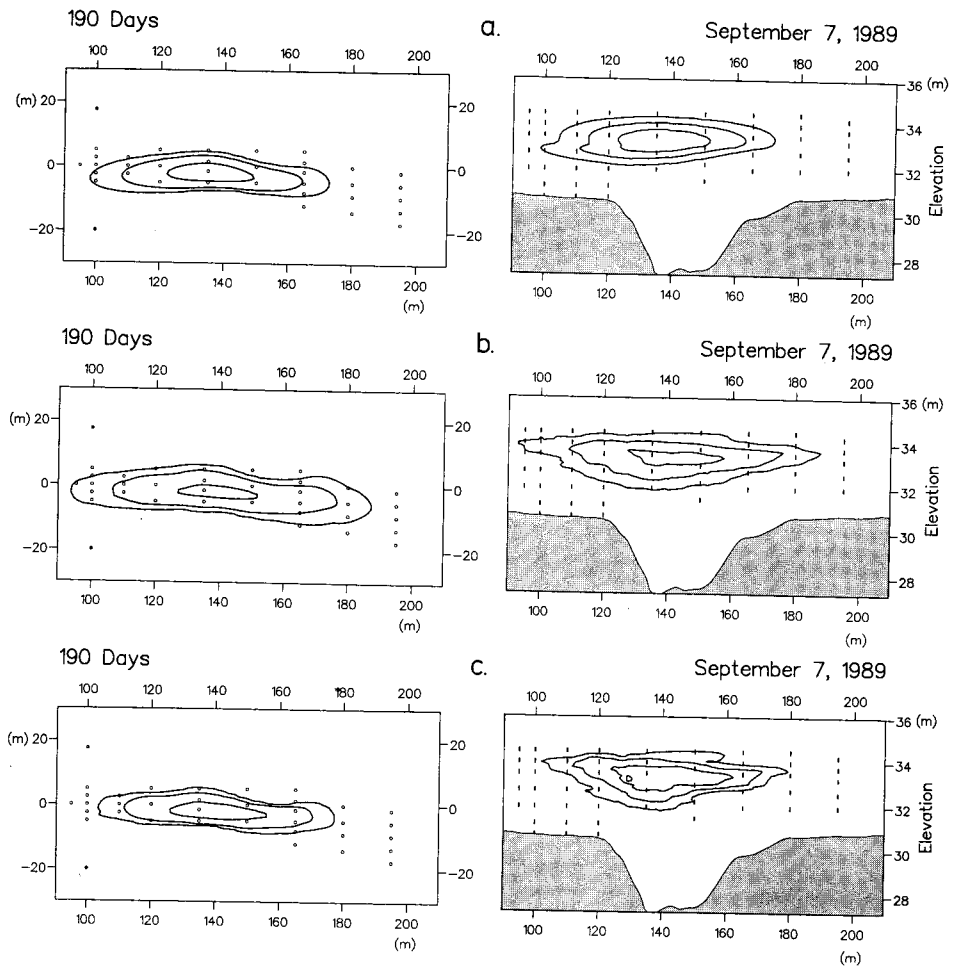

Fig. 19. Simulated horizontal distribution of "vertically averaged" tritium concentrations (left) and simulated vertical distribution (right). (*a*) Homogeneous three-layer model (α_{LH} = 0.45 m). (*b*) Heterogeneous three-layer model (α_{LH} = 0.45 m). (*c*) Heterogeneous three-layer model (α_{LH} = 0.01 m).

the homogeneous case were introduced. The simulations results after 190 days are compared in Figure 19; as is shown, the fluctuations of the generated ln K field have introduced some irregularities in the concentration distributions. However, the mean travel velocity and direction of the tracer plume are nearly the same in the two simulations. The longitudinal dimension of the plume is larger in the heterogeneous case, while the horizontal transverse and vertical dimensions of the plume have not increased significantly.

The increased dispersion in the heterogeneous case is due to the disturbances in the velocity field introduced by the fluctuations in the hydraulic conductivity field. In accordance with the higher resolution of the flow solution, lower values for the dispersivity parameters can be introduced. We made a few trial simulations with smaller values for the longitudinal horizontal dispersivity and as is also shown in Figure 19, a value of 0.01 m results in a dispersion pattern which is close to the observed pattern. This dispersivity represents the dispersion created by the heterogeneity at a scale below the scale of the numerical mesh.

7. Summary and Conclusions

A large-scale natural gradient tracer experiment for solute transport in groundwater was carried out in a sandy aquifer typical for the geological conditions in the western part of Denmark using tritium and chloride as tracers.

The aquifer at the site is unconfined with the water table located approximately 5 m below the ground surface. A low-permeable clay layer at an approximately 10 m depth defines the lower boundary. The water table fluctuated about 1.0 m over the season; however, all wells responded coherently and the flow direction therefore remained fairly constant during the experiment.

The statistical characteristics of the hydraulic conductivity distribution were determined on the basis of slug tests. Rather low values were obtained for both the variance of ln K (0.37) and the correlation length (in the range of 1.0–2.5 m).

A 200-m-long and 40-m-wide experimental area was designed with orientation along the groundwater flow direction. A dense three-dimensional piezometer network was established concurrently with the development of the tracer plumes in order to accurately determine the position of the tracers.

Tritium was selected as the primary tracer because of its detectability in low concentrations, and it proved very suitable for the experiment. In a second tracer experiment chloride together with other inorganic constituents was

injected. The chloride plume experienced a vertical displacement at the point of injection due to density contrasts and therefore this experiment was less suitable for detailed quantification of the dispersion characteristics.

Apart from the initial sinking of the chloride plume, both tracer plumes behaved similarly by showing predominant spreading in the longitudinal horizontal direction with very small spreading in the transverse horizontal and vertical directions.

The horizontal transport parameters were evaluated on the basis of breakthrough curves for vertically averaged tritium concentrations. For the travel distances examined (larger than 50 m) the dispersivities showed no significant trend with increased distance from the point of injection suggesting that the asymptotic stage was reached. The longitudinal dispersivity identified compared well to the value estimated on the basis of a stochastic theory of dispersion.

A numerical three-dimensional model was applied to the aquifer in order to better quantify the dispersivities. The model was coupled to a one-dimensional model for unsaturated flow to generate the seasonal variation of recharge to the water table. By assuming a three-layer structural geological model with uniform hydraulic properties, very accurate simulations were obtained of the seasonal fluctuations of the water table within the experimental area.

On the basis of a set of sensitivity simulations the following best fit dispersivity parameters were identified: α_{LH} = 0.45 m, α_{TH} = 0.001 m, and α_{TV} = 0.0005 m. The longitudinal horizontal dispersivity is of the same magnitude as found in the Borden and Cape Cod tracer experiments, while the transverse dispersivities in this experiment are smaller.

Using the dispersivities listed above, good agreement was obtained between the three-dimensional numerical simulations and observations of the overall behavior of both tracer plumes. On a more detailed scale, at the level of breakthrough curves in the individual piezometers, some discrepancies were present due to the disturbances created by local geological heterogeneities.

A single realization of the hydraulic conductivity field was generated using the turning band simulator to mimic the heterogeneity in the hydraulic properties. Because of the large transport distance involved in relation to the correlation scale of the fluctuations in the hydraulic conductivity, the single realization was presumed to be an analogue of the real aquifer. Due to the increased flow resolution it was possible to reduce the longitudinal dispersivity to a value of 0.01 m which consequently represents the dispersion created by the heterogeneity at a scale below the modeling scale.

The study shows that a deterministic advection-dispersion based three-dimensional numerical model in which the different structural geological layers are defined gives accurate predictions of the overall plume behavior in the investigated aquifer of alluvial origin for very small values of the dispersivities. This finding is of practical significance when dealing with aquifers composed of relatively homogeneous sandy outwash as the one investigated in this study. For more heterogeneous aquifers of more complicated geological structure and with a much higher hydraulic conductivity variance it is doubtful that the use of three-dimensional deterministic models would be adequate.

Acknowledgments. The Danish Isotope Center is acknowledged for obtaining the permission to use tritium as a tracer and for carrying out the injection and the initial tritium analyses. The Danish Hydraulic Institute is acknowledged for allowing us to apply the SHE model. Kenneth L. Kipp from the U.S. Geological Survey is gratefully acknowledged for his critical review and valuable comments to the manuscript.

REFERENCES

Ababou, R., L. W. Gelhar, and D. McLaughlin, Three-dimensional flow in random porous media, *Rep. 318*, Ralph M. Parsons Lab., Mass. Inst. of Technol., Cambridge, 1988.

American Public Health Association, *Standard Methods for the Examination of Water and Wastewater*, 16th ed., Washington, D. C., 1985.

Anderson, M. P., Using models to simulate the movement of contaminants through groundwater flow systems, *Crit. Rev. Environ. Control*, *9*, 97–156, 1979.

Bear, J., *Dynamics of Fluids in Porous Media*, 764 pp., Elsevier, New York, 1972.

Bear, J., *Hydraulics of Groundwater*, 569 pp., McGraw-Hill, New York, 1979.

Bjerg, P. L., and T. H. Christensen, A field experiment on cation exchange–affected solute transport in a sandy aquifer, *J. Contam. Hydrol.*, in press, 1993.

Bjerg, P. L., K. Hinsby, T. H. Christensen, and P. Gravesen, Spatial variability of hydraulic conductivity of an unconfined sandy aquifer determined by a mini slug test, *J. Hydrol.*, *136*, 107–122, 1992.

Boggs, J. M., S. C. Young, L. M. Beard, L. W. Gelhar, K. R. Rehfeldt, and E. E. Adams, Field study of dispersion in a heterogeneous aquifer, 1, Overview and site description, *Water Resour. Res.*, *28*(12), 3281–3291, 1992.

Dagan, G., Stochastic modeling of groundwater flow by unconditional and conditional probabilities, 2, The solute transport, *Water Resour. Res.*, *18*(4), 835–848, 1982.

Dagan, G., Solute transport in heterogeneous porous formations, *J. Fluid Mech.*, *145*, 157–177, 1984.

Danish Hydraulic Institute, A three-dimensional module for groundwater flow and solute transport in the SHE, internal research report, Dan. Hydraul. Inst., Horsholm, 1992.

Davis, S. N., D. Campbell, H. W. Bentley, and T. J. Flynn, *Groundwater Tracers*, 200 pp., National Water Well Association, Worthington, Ohio, 1985.

Dax, A., A note on the analysis of slugtests, *J. Hydrol.*, *91*, 153–177, 1987.

Freeze, R. A., and J. A. Cherry, *Groundwater*, Prentice-Hall, Englewood Cliffs, N. J., 1979.

Freyberg, D. L., A natural gradient experiment on solute transport in sand aquifer, 2, Spatial moments and the advection and dispersion of nonreactive tracers, *Water Resour. Res.*, *22*(13), 2031–2046, 1986.

Frind, E. O, W. H. M. Duynisveld, O. Strebel, and J. Boettcher, Simulation of nitrate and sulfate transport and transformation in the Fuhrberger Feld aquifer, Hannover, Germany, in *Contaminant Transport in Groundwater*, edited by H. E. Kobus and W. Kinzelbach, pp. 97–104, A. A. Balkema, Rotterdam, Netherlands, 1989.

Garabedian, S. P., L. W. Gelhar, and M. A. Celia, Large-scale dispersive transport in aquifers: Field experiments and reactive transport theory, *Rep. 315*, 280 pp., Ralph M. Parsons Lab., Mass. Inst. of Technol., Cambridge, 1988.

Garabedian, S. P., D. R. LeBlanc, L. W. Gelhar, and M. A. Celia, Large-scale natural gradient tracer test in sand and gravel, Cape Cod, Massachusetts, 2, Analysis of spatial moments for nonreactive tracer, *Water Resour. Res.*, *27*(5), 911–924, 1991.

Gaspar, E., and M. Oncescu, *Radioactive Tracers in Hydrology*, 342 pp., Elsevier, New York, 1972.

Gelhar, L. W., and C. L. Axness, Three-dimensional stochastic analysis of macrodispersion in aquifers, *Water Resour. Res.*, *19*(1), 161–180, 1983.

Gelhar, L. W., A. L. Gutjahr, and R. L. Naff, Stochastic analysis of macrodispersion in a stratified aquifer, *Water Resour. Res.*, *15*(6), 1387–1397, 1979.

Gelhar, L. W., A. Mantoglou, C. Welty, and K. R. Rehfeldt, A

review of field scale physical solute transport processes in saturated and unsaturated porous media, *Rep. EPRI EA-4190*, 116 pp., Electr. Power Res. Inst., Palo Alto, Calif., 1985.

Gilham, R. W., and J. A. Cherry, Contaminant migration in saturated unconsolidated geologic deposits, *Spec. Pap. Geol. Soc. Am.*, *189*, 31–62, 1982.

Hess, K. M., S. H. Wolf, M. A. Celia, and S. P. Garabedian, Macrodispersion and spatial variability of hydraulic conductivity in a sand and gravel aquifer, Cape Cod, Massachusetts, *Environ. Res. Brief EPA/600/M-91/005*, Environ. Prot. Agency, Ada, Okla., 1991.

Hinsby, K., P. L. Bjerg, L. J. Andersen, B. Skov, and E. V. Clausen, A mini slug test method for determination of a local hydraulic conductivity of an unconfined sandy aquifer, *J. Hydrol.*, *136*, 87–106, 1992.

Jensen, K. H., Simulation of water flow in the unsaturated zone including the root zone, *Ser. Pap. 33*, Inst. of Hydrodyn. and Hydraul. Eng., Tech. Univ. of Denmark, Lyngby, 1983.

Jensen, K. H., A. Refsgaard, and K. Bitsch, Mathematical modelling of contaminant transport from Vejen landfill (in Danish), *Rep. M1/M2*, Landfill Proj., Danish Environ. Prot. Agency, Copenhagen, 1991.

Killey, R. W. D., and G. L. Moltyaner, Twin Lake tracer tests: Setting, methodology, and hydraulic conductivity distribution, *Water Resour. Res.*, *24*(10), 1585–1612, 1988.

Kinzelbach, W., *Groundwater Modelling, An Introduction With Sample Programmes in BASIC*, 312 pp., Elsevier, New York, 1986.

Konikow, L. F., and J. D. Bredehoeft, Computer model of two-dimensional solute transport and dispersion in groundwater, in *Techniques of Water-Resources Investigations of the United States Geological Survey*, Chapter C2, Book 7, U.S. Geological Survey, Reston, Va., 1978.

Lallemand-Barres, A., and P. Peaudecerf, Recherche des relations entre la valeur de la dispersivité macroscropique d'un milieu aquifére, ses autres caractéristiques et les conditions de mesure, *Bull. 4*, 2e Sér., Sec III, Bur. de Rech. Géol. et Minèr., Orleans, France, 1978.

LeBlanc, D. R., S. P. Garabedian, K. M. Hess, L. W. Gelhar, R. D. Quadri, K. G. Stollenwerk, and W. W. Wood, Large-scale gradient tracer test in sand and gravel, Cape Cod, Massachusetts, 1, Experimental design and observed tracer movement, *Water Resour. Res.*, *27*(5), 895–910, 1991.

Leland, D. F., and D. Hillel, A field study of solute dispersion in a shallow, unconfined aquifer, *Soil Sci. Soc. Am. J.*, *46*, 905–912, 1982.

Mackay, D. M., D. L. Freyberg, P. V. Roberts, and J. A. Cherry, A natural gradient experiment on solute transport in a sand aquifer, 1, Approach and overview of plume movement, *Water Resour. Res.*, *22*(13), 2017–2029, 1986.

Mantoglou, A., and J. L. Wilson, The turning bands method for simulation of random fields using line generation by a spectral method, *Water Resour. Res.*, *18*(5), 1379–1394, 1982.

Matheron, G., and G. de Marsily, Is transport in porous media always diffusive? A counter-example, *Water Resour. Res.*, *16*(5), 901–917, 1980.

Moltyaner, G. L., and R. W. D. Killey, Twin Lake tracer tests: Longitudinal dispersion, *Water Resour. Res.*, *24*(10), 1613–1627, 1988*a*.

Moltyaner, G. L., and R. W. D. Killey, Twin Lake tracer tests: Transverse dispersion, *Water Resour. Res.*, *24*(10), 1628–1637, 1988*b*.

Sauty, J. P., and W. Kinzelbach, On the identification of the parameters of groundwater mass transport, *Groundwater Flow and Quality Modelling*, edited by E. Custodio et al., pp. 33–56, D. Reidel, Hingham, Mass., 1988*a*.

Sauty, J. P. and W. Kinzelbach, Computer aided tracer test interpretation code "Catti," Users manual, IFN Inst. für Wasserbau, Stuttgart, Germany, 1988*b*.

Scheidegger, A. E., General theory of dispersion in porous media, *J. Geophys. Res.*, *66*(10), 3273–3278, 1961.

Schincariol, R. A., and F. W. Schwartz, An experimental investigation of variable density flow and mixing in homogeneous and heterogeneous media, *Water Resour. Res.*, *26*(10), 2317–2329, 1990.

Smith, L., and F. W. Schwartz, Mass transport, 1, A stochastic analysis of macroscopic dispersion, *Water Resour. Res.*, *16*(2), 303–313, 1980.

Sudicky, E. A., A natural gradient experiment on solute transport in a sand aquifer: Spatial variability of hydraulic conductivity and its role in the dispersion process, *Water Resour. Res.*, *22*(13), 2069–2082, 1986.

Sudicky, E. A., J. A. Cherry, and E. O. Frind, Migration of contaminants in groundwater at a landfill: A case study, 4, A natural-gradient dispersion test, *J. Hydrol.*, *63*, 81–108, 1983.

Sudicky, E. A., S. L. Schellenberg, and K. T. B. MacQuarrie, Assessment of the behaviour of conservative and biodegradable solutes in heterogeneous porous media, in *Dynamics of Fluids in Hierarchical Porous Media*, edited by J. H. Cushman, pp. 429–461, Academic, San Diego, Calif., 1990.

Thomas, R. G., Groundwater models, in Irrigation and Drainage, *Spec. Pap.*, *21*, Food Agric. Organ., United Nations, Rome, 1973.

Tompson, A. F. B., R. Ababou, and L. W. Gelhar, Application and use of the three-dimensional turning bands random field generator: Single realization problems, *Rep. 313*, Ralph M. Parsons Lab., Mass. Inst. of Technol., Cambridge, 1987.

UNESCO, *Aquifer Contamination and Protection*, Project 8.3. of the International Hydrology Programme, edited by R. E. Jackson, 440 pp., Paris, 1980.

Vested, H. J., P. Justesen, and L. Ekebjærg, Advection-diffusion modelling in three dimensions, *Appl. Math. Modell.*, *12*, 506–519, 1992.

K. Bitsch and K. H. Jensen, ISVA, Institute of Hydrodynamics and Hydraulic Engineering, Technical University of Denmark, Building 115, DK-2800 Lyngby, Denmark.

P. L. Bjerg, Department of Environmental Engineering, Groundwater Research Centre, Technical University of Denmark, DK-2800 Lyngby, Denmark.

(Received March 26, 1992;
revised September 24, 1992;
accepted October 13, 1992.)